



TECH BRIEFS

NATIONAL AERONAUTICS AND SPACE ADMINISTRATION

-  **Technology Focus**
-  **Electronics/Computers**
-  **Software**
-  **Materials**
-  **Mechanics/Machinery**
-  **Manufacturing**
-  **Bio-Medical**
-  **Physical Sciences**
-  **Information Sciences**
-  **Books and Reports**

INTRODUCTION

Tech Briefs are short announcements of innovations originating from research and development activities of the National Aeronautics and Space Administration. They emphasize information considered likely to be transferable across industrial, regional, or disciplinary lines and are issued to encourage commercial application.

Additional Information on NASA Tech Briefs and TSPs

Additional information announced herein may be obtained from the NASA Technical Reports Server: <http://ntrs.nasa.gov>.

Please reference the control numbers appearing at the end of each Tech Brief. Information on NASA's Innovative Partnerships Program (IPP), its documents, and services is available on the World Wide Web at <http://www.ipp.nasa.gov>.

Innovative Partnerships Offices are located at NASA field centers to provide technology-transfer access to industrial users. Inquiries can be made by contacting NASA field centers listed below.

NASA Field Centers and Program Offices

Ames Research Center

Mary Walsh
(650) 604-1405
mary.w.walsh@nasa.gov

Dryden Flight Research Center

Ron Young
(661) 276-3741
ronald.m.young@nasa.gov

Glenn Research Center

Joe Shaw
(216) 977-7135
robert.j.shaw@nasa.gov

Goddard Space Flight Center

Nona Cheeks
(301) 286-5810
nona.k.cheeks@nasa.gov

Jet Propulsion Laboratory

Indrani Graczyk
(818) 354-2241
indrani.graczyk@jpl.nasa.gov

Johnson Space Center

John E. James
(281) 483-3809
john.e.james@nasa.gov

Kennedy Space Center

David R. Makufka
(321) 867-6227
david.r.makufka@nasa.gov

Langley Research Center

Michelle Ferebee
(757) 864-5617
michelle.t.ferebee@nasa.gov

Marshall Space Flight Center

Jim Dowdy
(256) 544-7604
jim.dowdy@nasa.gov

Stennis Space Center

Ramona Travis
(228) 688-3832
ramona.e.travis@ssc.nasa.gov

NASA Headquarters

Innovative Partnerships Office

Doug Comstock, Director
(202) 358-2221
doug.comstock@nasa.gov

Daniel Lockney,
Technology Transfer Lead
(202) 358-2037
daniel.p.lockney@nasa.gov

Small Business Innovation Research (SBIR) & Small Business Technology Transfer (STTR) Programs

Carl Ray, Program Executive
(202) 358-4652
carl.g.ray@nasa.gov



TECH BRIEFS

NATIONAL AERONAUTICS AND SPACE ADMINISTRATION

5 Technology Focus: Test & Measurement

- 5 Fused Reality for Enhanced Flight Test Capabilities
- 5 Thermography to Inspect Insulation of Large Cryogenic Tanks
- 6 Crush Test Abuse Stand
- 6 Test Generator for MATLAB Simulations
- 6 Dynamic Monitoring of Cleanroom Fallout Using an Air Particle Counter
- 7 Enhancement to Non-Contacting Stress Measurement of Blade Vibration Frequency

9 Electronics/Computers

- 9 Positively Verifying Mating of Previously Unverifiable Flight Connectors
- 9 Radiation-Tolerant Intelligent Memory Stack — RTIMS
- 10 Ultra-Low-Dropout Linear Regulator
- 10 Excitation of a Parallel Plate Waveguide by an Array of Rectangular Waveguides
- 11 FPGA for Power Control of MSL Avionics
- 11 UAVSAR Active Electronically Scanned Array
- 11 Lockout/Tagout (LOTO) Simulator

13 Manufacturing & Prototyping

- 13 Silicon Carbide Mounts for Fabry-Perot Interferometers
- 13 Measuring the In-Process Figure, Final Prescription, and System Alignment of Large Optics and Segmented Mirrors Using Lidar Metrology

15 Materials & Coatings

- 15 Fiber-Reinforced Reactive Nano-Epoxy Composites
- 15 Polymerization Initiated at the Sidewalls of Carbon Nanotubes
- 15 Metal-Matrix/Hollow-Ceramic-Sphere Composites
- 16 Piezoelectrically Enhanced Photocathodes
- 16 Iridium-Doped Ruthenium Oxide Catalyst for Oxygen Evolution
- 17 Improved Mo-Re VPS Alloys for High-Temperature Uses

19 Green Design

- 19 Data Service Provider Cost Estimation Tool
- 19 Hybrid Power Management-Based Vehicle Architecture

21 Mechanics/Machinery

- 21 Force Limit System
- 21 Levitated Duct Fan (LDF) Aircraft Auxiliary Generator
- 22 Compact, Two-Sided Structural Cold Plate Configuration
- 22 AN Fitting Reconditioning Tool
- 23 Active Response Gravity Offload System

25 Bio-Medical

- 25 Method and Apparatus for Forming Nanodroplets
- 25 Rapid Detection of the Varicella Zoster Virus in Saliva
- 26 Improved Devices for Collecting Sweat for Chemical Analysis

27 Physical Sciences

- 27 Phase-Controlled Magnetic Mirror for Wavefront Correction
- 27 Frame-Transfer Gating Raman Spectroscopy for Time-Resolved Multiscalar Combustion Diagnostics
- 28 Thermal Properties of Microstrain Gauges Used for Protection of Lithium-Ion Cells of Different Designs
- 29 In-Service Monitoring of Steam Pipe Systems at High Temperatures
- 30 Control Program and Optical Improvements of Fresnel Microspectrometer
- 30 Miniature Laser Magnetometer

33 Information Sciences

- 33 Finding Every Root of a Broad Class of Real, Continuous Functions in a Given Interval
- 33 Kalman Orbit Optimized Loop Tracking
- 34 Development of Jet Noise Power Spectral Laws

This document was prepared under the sponsorship of the National Aeronautics and Space Administration. Neither the United States Government nor any person acting on behalf of the United States Government assumes any liability resulting from the use of the information contained in this document, or warrants that such use will be free from privately owned rights.

35 Software

- 35 GLobal Integrated Design Environment
- 35 SSC Engineering Analysis
- 35 Automated Cryocooler Monitor and Control System Software
- 36 Common Bolted Joint Analysis Tool
- 36 Draper Station Analysis Tool
- 36 Commercial Modular Aero-Propulsion System Simulation 40k
- 37 The Planning Execution Monitoring Architecture
- 37 Jitter Controller Software
- 38 μ Shell Minimalist Shell for Xilinx Microprocessors
- 38 Software Displays Data on Active Regions of the Sun
- 39 InSAR Scientific Computing Environment
- 40 Software Architecture to Support the Evolution of the ISRU RESOLVE Engineering Breadboard Unit 2 (EBU2)
- 40 Coastal On-line Assessment and Synthesis Tool 2.0
- 41 Generalized Software Architecture Applied to the Continuous Lunar Water Separation Process and the Lunar Greenhouse Amplifier
- 42 Graphical Language for Data Processing
- 42 Monitoring Areal Snow Cover Using NASA Satellite Imagery
- 43 Adaptation of G-TAG Software for Validating Touch-and-Go Comet Surface Sampling Design Methodology
- 44 Onboard Short Term Plan Viewer
- 44 Multidisciplinary Tool for Systems Analysis of Planetary Entry, Descent, and Landing
- 44 Bundle Security Protocol for ION
- 45 Visual PEF Reader — VIPER
- 46 Link Analysis in the Mission Planning Lab
- 46 MatchGUI: A Graphical MATLAB-Based Tool for Automatic Image Co-Registration
- 47 Spacecraft Guidance, Navigation, and Control Visualization Tool
- 47 Mission Operations Planning and Scheduling System (MOPSS)
- 48 Global Precipitation Mission Visualization Tool
- 48 Thermal Protection System Imagery Inspection Management System —TIIMS
- 49 Computer-Aided Parallelizer and Optimizer
- 49 CCSDS Advanced Orbiting Systems Virtual Channel Access Service for QoS MACHETE Model
- 50 Conceptual Model of Quantities, Units, Dimensions, and Values
- 51 Sptrace
- 51 S-Band POSIX Device Drivers for RTEMS
- 51 MaROS: Information Management Service
- 52 Interplanetary Overlay Network Bundle Protocol Implementation
- 52 STRS SpaceWire FPGA Module
- 53 Geodetic Strain Analysis Tool



Fused Reality for Enhanced Flight Test Capabilities

Complex maneuvers can be accomplished without additional aircraft resources or risk.

Dryden Flight Research Center, Edwards, California

The feasibility of using Fused Reality-based simulation technology to enhance flight test capabilities has been investigated. In terms of relevancy to piloted evaluation, there remains no substitute for actual flight tests, even when considering the fidelity and effectiveness of modern ground-based simulators. In addition to real-world cueing (vestibular, visual, aural, environmental, etc.), flight tests provide subtle but key intangibles that cannot be duplicated in a ground-based simulator. There is, however, a cost to be paid for the benefits of flight in terms of budget, mission complexity, and safety, including the need for ground and control-room personnel, additional aircraft, etc.

A Fused Reality™ (FR) Flight system was developed that allows a virtual environment to be integrated with the test aircraft so that tasks such as aerial refueling, formation flying, or approach and landing can be accomplished without additional aircraft resources or the risk of operating in close proximity to the ground or other aircraft. Furthermore, the dynamic motions of the simulated objects

can be directly correlated with the responses of the test aircraft. The FR Flight system will allow real-time observation of, and manual interaction with, the cockpit environment that serves as a frame for the virtual out-the-window scene.

FR is a mixed-reality approach that employs four technologies: live video capture, real-time video editing, machine vision, and virtual environment simulation. Video from the trainee's perspective is sent to a processor that preserves pixels in the near-space environment (i.e., cockpit), and makes transparent the far-space environment (outside the cockpit windows) pixels using blue-screen imaging techniques. This bitmap is overlaid on a virtual environment and sent to the trainee's helmet-mounted display (HMD). The user can directly view and interact with the physical environment, while the simulated outside world serves as an interactive backdrop.

The system employs a head-mounted camera and display assembly, where the camera captures live video from the user's perspective and sends it to a computer for processing. The window frames

of the cockpit are bordered with colored tape, and when these color-coded borders are sensed, the computer keys out pixels lying within each window so that an underlying virtual scene is seen in place of the window pixels. The virtual simulation reacts to the user's head motion and control inputs, and the two layers — processed video and virtual scene — are combined and viewed by the user through a head-mounted display.

Critical hardware challenges included selection of color and material of the window bordering material, and identifying a lens filter to allow machine color recognition in the presence of bright sunlight. Software challenges included accommodating for every possible view (of one or more window borders), balancing sensor noise-smoothing against precision loss, and creating a means for rapidly calibrating color sensing thresholds for a given lighting environment.

This work was done by Ed Bachelder and David Klyde of Systems Technology, Inc. for Dryden Flight Research Center. Further information is contained in a TSP (see page 1). DRC-010-033

Thermography to Inspect Insulation of Large Cryogenic Tanks

Significant cost and schedule savings may be realized.

John F. Kennedy Space Center, Florida

Thermography has been used in the past to monitor active, large, cryogenic storage tanks. This approach proposes to use thermography to monitor new or refurbished tanks, prior to filling with cryogenic liquid, to look for insulation voids. Thermography may provide significant cost and schedule savings if voids can be detected early before a tank is returned to service.

The Launch Complex 39 Pad B liquid hydrogen storage tank at Kennedy Space Center has had performance issues since it was put into service in 1965. The loss rate from the Pad B tank was two to three times more than the

Pad A tank, which has resulted in a significant cumulative loss of hydrogen over more than 40 years of service. It has been theorized for years that the performance degradation was due to an insulation void; however, because of the cost and schedule disruption that would be required to fix the problem, it remained in service until Pad B was turned over after its support for the Shuttle program was finished. With the tank taken out of active service, it was confirmed that a major insulation void was present.

Because of the large thermal mass of the inner and outer spheres, heat trans-

fer between surfaces to equalize temperatures can be relatively slow, even when the temperature differences between the spheres themselves is small. Therefore, thermography has been suggested as an aid in acceptance testing of the tanks before cryogen is introduced to any tank, new or refurbished.

Models suggest that areas without insulation will heat less rapidly under solar illumination than areas with insulation, due to better thermal contact with the inner storage sphere. The resulting temperature difference across the outer shell of the tank should be a few degrees Celsius, which can be easily

visualized by off-the-shelf long-wave and mid-wave cameras.

The opportunity to test this theory presented itself over the last year as the Launch Complex 39 hydrogen tank was taken out of service in order to complete weld repairs.

The ability to detect insulation voids prior to filling with cryogen will save money and time, eliminating the expense of losing cryogen and the months required for chilling down and warming up the tank if a void is discovered after the cryogen is introduced

into the system. Potential savings could be in the millions if large voids are detected early.

This work was done by Ellen Arens and Robert Youngquist of Kennedy Space Center. Further information is contained in a TSP (see page 1). KSC-13575

Crush Test Abuse Stand

This technology can be used in most applications for the performance of battery testing.

Lyndon B. Johnson Space Center, Houston, Texas

The purpose of this system is to simulate an internal short on battery cells by causing deformation (a crushing force) in a cell without penetration. This is performed by activating a hydraulic cylinder on one side of a blast wall with a hydraulic pump located on the other. The operator can control the rate of the crush by monitoring a local pressure gauge connected to the hydraulic cylinder or a load cell digital display located at the hydraulic pump control area. The internal short simulated would be considered a worst-case scenario of a manufacturer's defect. This is a catastrophic failure of a cell and could be a very destructive event.

Fully charged cells are to have an internal short simulated at the center of the length of the cell (away from terminals). The crush can be performed with a ¼- to 1-in. (≈0.6- to 2.5-cm) rod placed crossways to the cell axis, causing deformation of the cell without penetration. The OCV (open-circuit voltage) and temperature of the cells, as well as the pressure and crushing force, are recorded during the operation. Occurrence of an internal short accompanied by any visible physical changes such as venting, fires, or explosions is reported. Typical analytical data examined after the test would be plots of voltage, temperature, and pressure or force versus time.

The rate of crushing force can be increased or decreased based on how fast the operator pumps the hydraulic pump. The size of cylinder used to compress the battery cell can be easily changed by adding larger or smaller fittings onto the end of the hydraulic cylinder based on the battery/cell size being tested. The cell is crushed remotely and videotaped, allowing the operator to closely monitor the situation from a safe distance.

This work was done by Jacob Collins, Judith Jeevarajan, and Mike Salinas of Johnson Space Center. For further information, contact the JSC Innovation Partnerships Office at (281) 483-3809. MSC-23700-1

Test Generator for MATLAB Simulations

Goddard Space Flight Center, Greenbelt, Maryland

MATLAB Automated Test Tool, version 3.0 (MATT 3.0) is a software package that provides automated tools that reduce the time needed for extensive testing of simulation models that have been constructed in the MATLAB programming language by use of the Simulink and Real-Time Workshop programs. MATT 3.0 runs on top of the

MATLAB engine application-program interface to communicate with the Simulink engine. MATT 3.0 automatically generates source code from the models, generates custom input data for testing both the models and the source code, and generates graphs and other presentations that facilitate comparison of the outputs of the models and the

source code for the same input data. Context-sensitive and fully searchable help is provided in HyperText Markup Language (HTML) format.

This program was written by Joel Henry of the University of Montana for Goddard Space Flight Center. Further information is contained in a TSP (see page 1). GSC-14861-1

Dynamic Monitoring of Cleanroom Fallout Using an Air Particle Counter

Goddard Space Flight Center, Greenbelt, Maryland

The particle fallout limitations and periodic allocations for the James Webb Space Telescope are very stringent. Standard prediction methods are complicated by non-linearity and monitor-

ing methods that are insufficiently responsive. A method for dynamically predicting the particle fallout in a cleanroom using air particle counter data was determined by numerical correlation.

This method provides a simple linear correlation to both time and air quality, which can be monitored in real time. The summation of effects provides the program better understanding of the

cleanliness and assists in the planning of future activities.

Definition of fallout rates within a cleanroom during assembly and integration of contamination-sensitive hardware, such as the James Webb Space Telescope, is essential for budgeting purposes. Balancing the activity levels for assembly and test with the particle accumulation rate is paramount. The current approach to predicting particle fallout in a cleanroom assumes a constant

air quality based on the rated class of a cleanroom, with adjustments for projected work or exposure times. Actual cleanroom class can also depend on the number of personnel present and the type of activities.

A linear correlation of air quality and normalized particle fallout was determined numerically. An air particle counter (standard cleanroom equipment) can be used to monitor the air quality on a real-time basis and deter-

mine the “class” of the cleanroom (per FED-STD-209 or ISO-14644). The correlation function provides an area coverage coefficient per class-hour of exposure. The prediction of particle accumulations provides scheduling inputs for activity levels and cleanroom class requirements.

This work was done by Radford Perry of Goddard Space Flight Center. Further information is contained in a TSP (see page 1). GSC-16108-1

Enhancement to Non-Contacting Stress Measurement of Blade Vibration Frequency

John H. Glenn Research Center, Cleveland, Ohio

A system for turbo machinery blade vibration has been developed that combines time-of-arrival sensors for blade vibration amplitude measurement and radar sensors for vibration frequency and mode identification. The enabling technology for this continuous blade monitoring system is the radar sensor, which provides a continuous time series of blade displacement over a portion of a revolution. This allows the

data reduction algorithms to directly calculate the blade vibration frequency and to correctly identify the active modes of vibration.

The work in this project represents a significant enhancement in the mode identification and stress calculation accuracy in non-contacting stress measurement system (NSMS) technology when compared to time-of-arrival measurements alone.

This work was done by Michael Platt and John Jagodnik of Mechanical Solutions for Glenn Research Center. Further information is contained in a TSP (see page 1).

Inquiries concerning rights for the commercial use of this invention should be addressed to NASA Glenn Research Center, Innovative Partnerships Office, Attn: Steven Fedor, Mail Stop 4-8, 21000 Brookpark Road, Cleveland, Ohio 44135. Refer to LEW-18602-1.



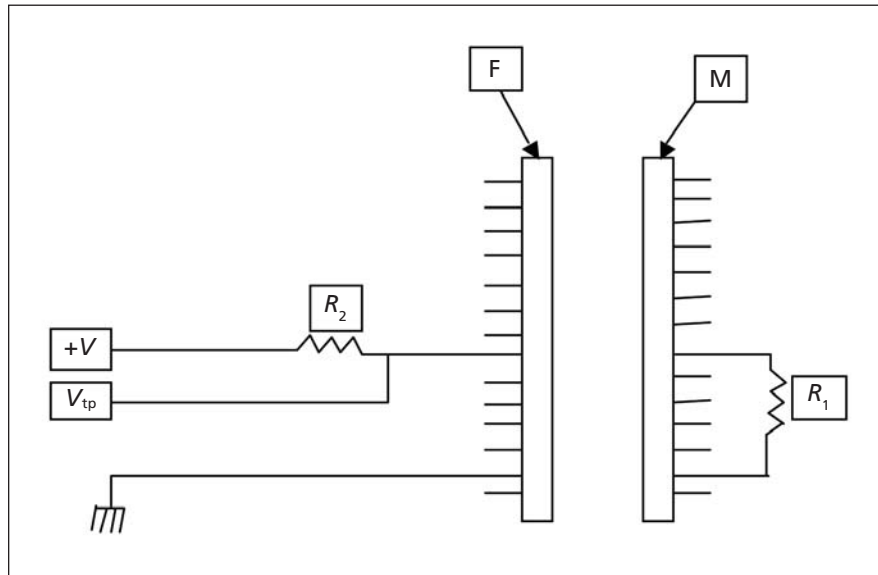
Positively Verifying Mating of Previously Unverifiable Flight Connectors

New approach ensures secure connections.

Goddard Space Flight Center, Greenbelt, Maryland

Current practice is to uniquely key the connectors, which, when mated, could not be verified by ground tests such as those used in explosive or non-explosive initiators and pyro valves. However, this practice does not assure 100-percent correct mating. This problem could be overcome by the following approach.

Errors in mating of interchangeable connectors can result in degraded or failed space mission. Mating of all flight connectors considered not verifiable via ground tests can be verified electrically by the following approach. It requires two additional wires going through the connector of interest, a few resistors, and a voltage source (see figure). The test-point voltage V_{tp} when the connector is not mated will be the same as the input voltage, which gets attenuated by the resistor R_1 when the female (F) and male (M) connectors are mated correctly and properly. The voltage at the test point will be a function of R_1 and R_2 . Monitoring of the test point could be done on ground support equipment (GSE) only, or it can be a telemetry point. For implementation on multiple connector pairs, a different value for R_1 or R_2 or both can be selected for each pair of connectors



The basic Circuit Diagram for verifying secure connection.

that would result in a unique test point voltage for each connector pair. Each test point voltage is unique, and correct test point voltage is read only when the correct pair is mated correctly together. Thus, this design approach can be used to verify positively the correct mating of

the connector pairs. This design approach can be applied to any number of connectors on the flight vehicle.

This work was done by R.K. Chetty Pandipati and Marlon Enciso of Goddard Space Flight Center. Further information is contained in a TSP (see page 1). GSC-15896-1

Radiation-Tolerant Intelligent Memory Stack — RTIMS

RTIMS can be used in real-time data processing, reconfigurable computing, and memory-intensive applications.

Langley Research Center, Hampton, Virginia

This innovation provides reconfigurable circuitry and 2-Gb of error-corrected or 1-Gb of triple-redundant digital memory in a small package. RTIMS uses circuit stacking of heterogeneous components and radiation shielding technologies. A reprogrammable field-programmable gate array (FPGA), six synchronous dynamic random access memories, linear regulator, and the radiation mitigation circuits are stacked

into a module of 42.7×42.7×13 mm. Triple module redundancy, current limiting, configuration scrubbing, and single-event function interrupt detection are employed to mitigate radiation effects. The novel self-scrubbing and single event functional interrupt (SEFI) detection allows a relatively “soft” FPGA to become radiation tolerant without external scrubbing and monitoring hardware.

RTIMS enables significant reductions in the size and mass of mission memory arrays, and is a radiation-tolerant memory suitable for both GEO and LEO space missions through the use of new package-level radiation shielding technology and triple modular redundancy (TMR) FPGA techniques. RTIMS also provides a simplified interface to a large SDRAM (synchronous dynamic random access memory) array with

built-in logic for timing reads, writes, and refresh cycles.

Mission flexibility is added by operating the memory array in the TMR architecture with 1 Gb of storage or in an EDAC (Error Detection And Correction) mode where part of the memory is used to detect and correct errors with 2 Gb of storage (corrects single bit errors and detects double bit errors). This allows RTIMS to be used effectively on many types of missions, because it can be configured for the "harshness" of the expected environment.

RTIMS enables in-flight reconfigurability by using SRAM (static random access memory)-based FPGA technology.

The design overcomes both hardware and software errors that may be detected after launch during mission operations. This reduces overall mission risk, which is increasingly important as flight system development times and budgets decrease. It also allows RTIMS to adapt to changing mission conditions.

The design increases system reliability by distributing the radiation mitiga-

tion structure to each component instead of to a singlepoint failure at the system level. The mitigation techniques significantly simplify system design. RTIMS is well suited for deployment in real-time data processing, reconfigurable computing, and memory-intensive applications.

This work was done by Tak-kwong Ng and Jeffrey A. Herath for Langley Research Center. Further information is contained in a TSP (see page 1). LAR-17257-1

Ultra-Low-Dropout Linear Regulator

Goddard Space Flight Center, Greenbelt, Maryland

A radiation-tolerant, ultra-low-dropout linear regulator can operate between -150 and 150 °C. Prototype components were demonstrated to be performing well after a total ionizing dose of 1 Mrad (Si). Unlike existing components, the linear regulator developed during this activity is unconditionally stable over all operating regimes without the need for an external compensation capacitor. The absence of an external capacitor reduces overall system mass/volume, increases reliability, and lowers cost.

Linear regulators generate a precisely controlled voltage for electronic circuits regardless of fluctuations in the load current that the circuit draws

from the regulator. To maximize the efficiency of the regulator, the dropout voltage (a measure of the voltage the regulator itself needs to operate) needs to be as small as possible. Existing regulators use p-channel transistors to minimize the dropout voltage, but p-channel regulators are intrinsically unstable and require an external compensation capacitor to stabilize their operation. The electrical properties of the compensation capacitor (in particular, its equivalent series resistance, ESR) must be well controlled to ensure stability. Changes in the ESR with temperature and/or radiation doses present challenges to stable reg-

ulator operation in extreme environments. This innovation allows an n-channel transistor to perform the regulation without the need for an external capacitor.

The n-channel pass transistor of the linear regulator operates in depletion mode thereby allowing ultralow dropout voltages of less than 100 mV.

This work was done by Trevor Thornton of Arizona State University and William Lepkowski and Seth Wilk of SJT Micropower for Goddard Space Flight Center. For further information, contact the Goddard Innovative Partnerships Office at (301) 286-5810. GSC-16097-1

Excitation of a Parallel Plate Waveguide by an Array of Rectangular Waveguides

NASA's Jet Propulsion Laboratory, Pasadena, California

This work addresses the problem of excitation of a parallel plate waveguide by an array of rectangular waveguides that arises in applications such as the continuous transverse stub (CTS) antenna and dual-polarized parabolic cylindrical reflector antennas excited by a scanning line source. In order to design the junction region between the parallel plate waveguide and the linear array of rectangular waveguides, waveguide sizes have to be chosen so that the input match is adequate for the range of scan angles for both polarizations.

Electromagnetic wave scattered by the junction of a parallel plate waveguide by an array of rectangular wave-

guides is analyzed by formulating coupled integral equations for the aperture electric field at the junction. The integral equations are solved by the method of moments. In order to make the computational process efficient and accurate, the method of weighted averaging was used to evaluate rapidly oscillating integrals encountered in the moment matrix. In addition, the real axis spectral integral is evaluated in a deformed contour for speed and accuracy. The MoM results for a large finite array have been validated by comparing its reflection coefficients with corresponding results for an infinite array generated by the commercial finite element code, HFSS. Once the aperture electric field is

determined by MoM, the input reflection coefficients at each waveguide port, and coupling for each polarization over the range of useful scan angles, are easily obtained.

Results for the input impedance and coupling characteristics for both the vertical and horizontal polarizations are presented over a range of scan angles. It is shown that the scan range is limited to about 35° for both polarizations and therefore the optimum waveguide is a square of size equal to about 0.62 free space wavelength.

This work was done by Sembiam Rengaranjan of Caltech for NASA's Jet Propulsion Laboratory. For more information, contact iaoffice@jpl.nasa.gov. NPO-47943

FPGA for Power Control of MSL Avionics

NASA's Jet Propulsion Laboratory, Pasadena, California

A PLGT FPGA (Field Programmable Gate Array) is included in the LCC (Load Control Card), GID (Guidance Interface & Drivers), TMC (Telemetry Multiplexer Card), and PFC (Pyro Firing Card) boards of the Mars Science Laboratory (MSL) spacecraft. (PLGT stands for PFC, LCC, GID, and TMC.) It provides the interface between the backside bus and the power drivers on these boards. The LCC drives power switches to switch power loads, and also relays. The GID drives the thrusters and latch valves, as well as having the star-tracker and Sun-sensor interface. The PFC

drives pyros, and the TMC receives digital and analog telemetry. The FPGA is implemented both in Xilinx (Spartan 3-400) and in Actel (RTSX72SU, ASX72S). The Xilinx Spartan 3 part is used for the breadboard, the Actel ASX part is used for the EM (Engineer Module), and the pin-compatible, radiation-hardened RTSX part is used for final EM and flight.

The MSL spacecraft uses a FC (Flight Computer) to control power loads, relays, thrusters, latch valves, Sun-sensor, and star-tracker, and to read telemetry such as temperature. Commands are sent

over a 1553 bus to the MREU (Multi-Mission System Architecture Platform Remote Engineering Unit). The MREU sends over a 'remote serial command bus' c-bus to the LCC, GID TMC, and PFC. The MREU also sends out telemetry addresses via a 'remote serial telemetry address bus' to the LCC, GID, TMC, and PFC, and the status is returned over the remote serial telemetry data bus.

This work was done by Duo Wang and Gary R. Burke of Caltech for NASA's Jet Propulsion Laboratory. For more information, contact iaoffice@jpl.nasa.gov. NPO-47022

UAVSAR Active Electronically Scanned Array

NASA's Jet Propulsion Laboratory, Pasadena, California

The Uninhabited Airborne Vehicle Synthetic Aperture Radar (UAVSAR) is a pod-based, L-band (1.26 GHz), repeat-pass, interferometric, synthetic aperture radar (InSAR) used for Earth science applications. Repeat-pass interferometric radar measurements from an airborne platform require an antenna that can be steered to maintain the same angle with respect to the flight track over a wide range of aircraft yaw angles.

In order to be able to collect repeat-pass InSAR data over a wide range of wind conditions, UAVSAR employs an active electronically scanned array (AESA). During data collection, the UAVSAR flight software continuously reads the aircraft attitude state measured by the Embedded GPS/INS system (EGI) and electronically steers the beam so that it remains perpendicular to the flight track throughout the data collection.

This work was done by Gregory A. Sadowy, Neil F. Chamberlain, Mark S. Zawadzki, Kyle M. Brown, Charles D. Fisher, Harry S. Figueroa, Gary A. Hamilton, Cathleen E. Jones, Vatche Vorperian, and Maurio B. Grando of Caltech for NASA's Jet Propulsion Laboratory. For more information, contact iaoffice@jpl.nasa.gov. NPO-47503

Lockout/Tagout (LOTO) Simulator

This tool can be used to train hands-on workers, safety personnel, and engineers writing LOTO procedures.

John F. Kennedy Space Center, Florida

The Lockout/Tagout (LOTO) Simulator is a portable training aid, or demonstration tool, designed to physically illustrate real-time critical-safety concepts of electrical lockout/tagout. The objective is to prevent misinterpretations of what is off and what is on during maintenance and repair of complex electrical systems. The simulator is designed in the form of a hinged box that opens up and stands on its own as an easel for demonstrations.

On the outer face of the unit is a simulated circuit breaker box housing the switches. The breakers control the main power to the unit, a light bulb, and an

electrical control cabinet. The light bulb is wired so that either of two breakers can provide power to it. When power is sent to the electrical control cabinet, a red indicator light illuminates.

Inside the cabinet is the power supply from a personal computer. The power supply produces a 12-V dc output that is sent over to a small fan next to it, also from a computer, and an amber light on the front of the cabinet illuminates. A separate switch powers the fan on and off. The power supply is behind a plastic shield to protect against exposure to live conductors. Electrical banana jacks are mounted in

the plastic shield to allow a voltmeter to be connected safely when opening the cabinet and taking a meter reading to verify de-energization as part of a simulation exercise.

This LOTO simulator prototype is designed and fabricated as an all-in-one unit. All accessories can be stored inside the hinged case, and there is a handle on top for ease of transport.

The circuit breaker labels attach with hook and loop fasteners so that they may be moved and changed to fit the training or demonstration scenario. The warning signs and labels on the electrical control box are magnetic, al-

lowing for easy reconfiguration to emulate different equipment setups. A specially designed magnetic cover was made to disguise the indicator lights for demonstrations when these indicators are not used. The cover is disguised as an arc flash safety label that would typically be found on such a cabinet.

One indicator light has a separate switch that can take it offline. This is to allow for demonstration to trainees on why it is important not to completely

rely on indicator lights, but that they should always take a meter reading at the exposed conductors to absolutely verify de-energization before exposure. A clear plastic barrier and banana jacks inside the cabinet provide a safe way to plug in a voltmeter for demonstrations without exposure to the hazards of energized equipment.

A small remote control unit is wired into the fan circuit. The remote allows the demonstrator to turn the fan on and

off, provided that all of the breakers and switches leading to it are configured on as well. The remote feature was added in order to demonstrate the importance of starting the lockout/tagout task with energized equipment, then powering it down, isolating it, and locking it out to ensure that the correct breakers have been locked out.

This work was done by Jennifer Scheer of Kennedy Space Center. Further information is contained in a TSP (see page 1). KSC-13389



☐ Silicon Carbide Mounts for Fabry-Perot Interferometers

Goddard Space Flight Center, Greenbelt, Maryland

Etalon mounts for tunable Fabry-Perot interferometers can now be fabricated from reaction-bonded silicon carbide structural components. These mounts are rigid, lightweight, and thermally stable. The fabrication of these mounts involves the exploitation of post-casting capabilities that (1) enable creation of monolithic structures having reduced (in comparison with prior such structures) degrees of material inhomogeneity and (2) reduce the need for fastening hardware and accommodations. Such silicon carbide mounts could be used to make lightweight Fabry-Perot interferometers or could

be modified for use as general lightweight optical mounts.

Heretofore, tunable Fabry-Perot interferometer structures, including mounting hardware, have been made from the low-thermal-expansion material Invar (a nickel/iron alloy) in order to obtain the thermal stability required for spectroscopic applications for which such interferometers are typically designed. However, the high mass density of Invar structures is disadvantageous in applications in which there are requirements to minimize mass.

Silicon carbide etalon mounts have been incorporated into a tunable

Fabry-Perot interferometer of a prior design that originally called for Invar structural components. The strength, thermal stability, and survivability of the interferometer as thus modified are similar to those of the interferometer as originally designed, but the mass of the modified interferometer is significantly less than the mass of the original version.

This work was done by Scott Lindemann of Michigan Aerospace Corp. for Goddard Space Flight Center. For further information, contact the Goddard Innovative Partnerships Office at (301) 286-5810. GSC-14957-1

☐ Measuring the In-Process Figure, Final Prescription, and System Alignment of Large Optics and Segmented Mirrors Using Lidar Metrology

This technique has application in commercial optics and lithography.

Goddard Space Flight Center, Greenbelt, Maryland

The fabrication of large optics is traditionally a slow process, and fabrication capability is often limited by measurement capability. While techniques exist to measure mirror figure with nanometer precision, measurements of large-mirror prescription are typically limited to submillimeter accuracy. Using a lidar instrument enables one to measure the optical surface rough figure and prescription in virtually all phases of fabrication without moving the mirror from its polishing setup. This technology improves the uncertainty of mirror prescription measurement to the micron-regime.

Furthermore, during instrument assembly, a lidar instrument measures the fabricated optical surface directly and compares with scans of diffuse, mechanical surfaces or other coordinate system references on metering structures. This speeds the alignment process and removes the necessity of ancillary alignment fiducials because the optical surface can be sampled directly.

The commercial lidar system illuminates a target surface with a focused, near-IR beam. The instrument collects scattered light returned from the target and optically mixes it with a reference signal maintained within the instrument, obtaining range data. The energy is directed from the instrument to any target within a field of regard spanning $>360^\circ$ in azimuth and $\pm 45^\circ$ in elevation and ranging ≈ 60 m. The uncertainty in range is typically ≈ 15 microns and < 1 arcsec in angle. Since the instrument can detect faint, scattered radiation, it can be used to detect errors directly in the surface figure and prescription of an optic during in-process fabrication, when the surface is rough. Since the surface will have a matt or ground finish, this measurement can be accomplished without necessarily locating the lidar instrument in any special location with respect to the mirror, as long as it has sufficient line of sight to the surface.

The lidar would scan the surface using a preprogrammed grid of sample points

that could be arbitrary or have a relationship to the mirror edges. As the mirror progresses through grinding into polishing phases, the surface becomes more specular. In order to detect fabrication errors in the figure and prescription at this stage, the lidar must be located close to the center of curvature of the optic. The tolerance for this location can be derived from the field of view of the lidar's camera and the approximate prescription of the optic under test, but is typically of-order centimeters. The lidar's camera similarly limits the detectable aspheric departure.

The location tolerance was generous and could be accomplished by locating the lidar unit using a simple tape measure. For mirrors with glass substrates, during lidar measurement in the polishing phase when the surface is approximately specular, one would need to apply a temporary coating to the surface under test using, e.g., a spray-on type coating applicator already in common use in optical shops. (Alternatively, cus-

tom software could be used to filter the range data to select the return from the dimmer surface.) Mirrors with metal substrates would need no such temporary coating during the lidar measurement in the polishing phase. Since the instrument can also detect bright, specularly returned radiation, it can be used to directly characterize the as-built prescription of large optics after polishing and coating. The lidar must be posi-

tioned near the center of curvature (but only to within the loose tolerance described above). The lidar would scan the surface using a preprogrammed grid of sample points.

In a similar manner, the lidar may be used for the coarse alignment and phasing of segmented telescope primary mirrors for future, large space- and ground-based observatories. Located near the nominal center of curvature,

the segments are scanned and iteratively aligned to microns, where other, interferometric or image-based techniques would be used to complete fine alignment.

This work was done by Raymond Ohl of Goddard Space Flight Center, Anthony Slotwinski of Pyxisvision, and Bente Eegholm and Babak Saif of the Space Telescope Science Institute. Further information is contained in a TSP (see page 1). GSC-15988-1



Fiber-Reinforced Reactive Nano-Epoxy Composites

Marshall Space Flight Center, Alabama

An ultra-high-molecular-weight polyethylene/matrix interface based on the fabrication of a reactive nano-epoxy matrix with lower surface energy has been improved. Enhanced mechanical properties versus pure epoxy on a three-point bend test include: strength (25 percent), modulus (20 percent), and toughness (30 percent). Increased thermal properties include higher T_g (glass transition temperature) and stable CTE (coefficient of thermal expansion). Improved processability for manufacturing

composites includes faster wetting rates on macro-fiber surfaces, lower viscosity, better resin infusion rates, and improved rheological properties. Improved interfacial adhesion properties with Spectra fibers by pullout tests include initial debonding force of 35 percent, a maximum pullout force of 25 percent, and energy to debond at 65 percent. Improved mechanical properties of Spectra fiber composites (tensile) aging resistance properties include hygrothermal effects.

With this innovation, high-performance composites have been created, including carbon fibers/nano-epoxy, glass fibers/nano-epoxy, aramid fibers/nano-epoxy, and ultra-high-molecular-weight polyethylene fiber (UHMWPE).

This work was done by Wei-Hong (Katie) Zhong of North Dakota State University for Marshall Space Flight Center. For further information, contact Sammy Nabors, MSFC Commercialization Assistance Lead, at sammy.a.nabors@nasa.gov. Refer to MFS-32666-1.

Polymerization Initiated at the Sidewalls of Carbon Nanotubes

Lyndon B. Johnson Space Center, Houston, Texas

A process has been developed for growing polymer chains via anionic, cationic, or radical polymerization from the side walls of functionalized carbon nanotubes, which will facilitate greater dispersion in polymer matrices, and will greatly enhance reinforcement ability in polymeric material.

Aryl bromide functionalized carbon nanotubes are dispersed in 5-mL tetrahydrofuran (THF), and a solution of n-butyllithium (5 mL, 2.19 M in hexane) was added at 23 °C, and the solution stirred for 10 min. The stirring was then turned off, and the nanotubes were allowed to settle out of solution. After settling, the excess n-butyllithium solution was removed from the reaction vessel via cannula, and the nanotubes were washed three times with dry THF (10 mL) to remove traces of n-butyllithium.

The flask was then charged with dry THF (10 mL), and the tubes were dispersed in solution with rapid stirring. Styrene (1.7 mL, 15 mmol) was added to the reaction vessel, and the mixture was stirred for 180 min before adding ethanol (1 mL) or a function terminator of choice such as trimethylsilyl chloride. The mixture was then diluted with 100 mL dichloromethane, and filtered through Fisherbrand P8 filter paper to remove any large particulates. The filtrate was concentrated under reduced pressure and precipitated into methanol. The resulting gray powder was then collected by filtration, using Whatman 451 filter paper and dried under vacuum (0.1 mm) to a constant weight (typically 0.100–1.00 g, depending on the precise amount of styrene added). This material can then be

blended with other polymers, or can be molded and used by itself as a specialty material.

This work was done by James M. Tour and Jared L. Hudson of Rice University for Johnson Space Center. For further information, contact the JSC Innovation Partnerships Office at (281) 483-3809.

In accordance with Public Law 96-517, the contractor has elected to retain title to this invention. Inquiries concerning rights for its commercial use should be addressed to:

*Rice University
Office of Technology Transfer
6100 Main Street
Houston, TX 77005
Phone No.: (713) 348-6188
E-mail: kbaez@rice.edu*

Refer to MSC-24065-1, volume and number of this NASA Tech Briefs issue, and the page number.

Metal-Matrix/Hollow-Ceramic-Sphere Composites

These materials are relatively inexpensive, lightweight, stiff, tailorable, and machinable.

Goddard Space Flight Center, Greenbelt, Maryland

A family of metal/ceramic composite materials has been developed that are relatively inexpensive, lightweight alternatives to structural materials that are typified by beryllium, aluminum,

and graphite/epoxy composites. These metal/ceramic composites were originally intended to replace beryllium (which is toxic and expensive) as a structural material for lightweight

mirrors for aerospace applications. These materials also have potential utility in automotive and many other terrestrial applications in which there are requirements for lightweight mate-

rials that have high strengths and other tailorable properties as described below.

The ceramic component of a material in this family consists of hollow ceramic spheres that have been formulated to be lightweight (0.5 g/cm^3) and have high crush strength [40–80 ksi (≈ 276 – 552 MPa)]. The hollow spheres are coated with a metal to enhance a specific performance — such as shielding against radiation (cosmic rays or x rays) or against electromagnetic interference at radio and lower frequencies, or a material to reduce the coefficient of thermal expansion (CTE) of the final composite material, and/or materials to mitigate any mismatch between the spheres and

the matrix metal. Because of the high crush strength of the spheres, the initial composite workpiece can be forged or extruded into a high-strength part. The total time taken in processing from the raw ingredients to a finished part is typically 10 to 14 days depending on machining required.

For purposes of further processing, the material behaves like a metal: It can be processed by conventional machining (including formation of threads) or electrical-discharge machining, and pieces of the material can be joined by techniques commonly used to join metal pieces. The material is also receptive to coating materials and exhibits highly variable thermal conductivity from

metal to ceramic depending on loading.

Typical mechanical properties of such a material include a density less than that of beryllium (ranging from 1.2 – 17 g/cm^3 while the density of beryllium is 1.85 g/cm^3) and modulus as high as 25 Msi (≈ 170 GPa). In contrast, the modulus of aluminum is generally 14 Msi (≈ 97 GPa). The CTE, the thermal conductivity, and the specific heat can be tailored, through the formulation of the ceramic and metal matrix ingredients of the composite.

This work was done by Dean M. Baker of Advanced Powder Solutions, Inc. for Goddard Space Flight Center. Further information is contained in a TSP (see page 1). GSC-15348-1

Piezoelectrically Enhanced Photocathodes

Attributes would include stability, high efficiency, and relative ease of fabrication.

NASA's Jet Propulsion Laboratory, Pasadena, California

Doping of photocathodes with materials that have large piezoelectric coefficients has been proposed as an alternative means of increasing the desired photoemission of electrons. Treating cathode materials to increase emission of electrons is called “activation” in the art. It has been common practice to activate photocathodes by depositing thin layers of suitable metals (usually, cesium). Because cesium is unstable in air, fabrication of cesiated photocathodes and devices that contain them must be performed in sealed tubes under vacuum. It is difficult and costly to perform fabrication processes in enclosed, evacuated spaces. The proposed piezoelectrically enhanced photocathodes would have electron-emission properties similar to those of cesiated photocathodes but would be stable in air, and therefore could be fabricated more easily and at lower cost.

Candidate photocathodes include nitrides of elements in column III of the periodic table — especially compounds of the general formula $\text{Al}_x\text{Ga}_{1-x}\text{N}$ (where $0 \leq x \leq 1$). These compounds have high piezoelectric coefficients and are suitable for obtaining response to ultraviolet light. Fabrication of a photocathode according to the proposal would include inducement of strain in cathode layers during growth of the layers on a substrate. The strain would be induced by exploiting structural mismatches among the various constituent materials of the cathode. Because of the piezoelectric effect in this material, the strain would give rise to strong electric fields that, in turn, would give rise to a high concentration of charge near the surface.

Examples of devices in which piezoelectrically enhanced photocathodes could be used include microchannel plates, electron-bombarded charge-coupled devices,

image tubes, and night-vision goggles. Piezoelectrically enhanced photocathode materials could also be used in making highly efficient monolithic photodetectors. Highly efficient and stable piezoelectrically enhanced, ultraviolet-sensitive photocathodes and photodetectors could be fabricated by use of novel techniques for growing piezoelectrically enhanced layers, in conjunction with thinning and dopant-selective etching techniques.

This work was done by Robert A. Beach, Shouleh Nikzad, Lloyd Douglas Bell, and Robert Strittmatter of Caltech for NASA's Jet Propulsion Laboratory. Further information is contained in a TSP (see page 1).

This invention is owned by NASA, and a patent application has been filed. Inquiries concerning nonexclusive or exclusive license for its commercial development should be addressed to the Patent Counsel, NASA Management Office—JPL. Refer to NPO-40407.

Iridium-Doped Ruthenium Oxide Catalyst for Oxygen Evolution

Possible applications of this catalyst include fabrication of water electrolysis units in hydrogen generators.

NASA's Jet Propulsion Laboratory, Pasadena, California

NASA requires a durable and efficient catalyst for the electrolysis of water in a polymer-electrolyte-membrane (PEM) cell. Ruthenium oxide in a slightly reduced form is known to be a very effi-

cient catalyst for the anodic oxidation of water to oxygen, but it degrades rapidly, reducing efficiency. To combat this tendency of ruthenium oxide to change oxidation states, it is combined with irid-

ium, which has a tendency to stabilize ruthenium oxide at oxygen evolution potentials. The novel oxygen evolution catalyst was fabricated under flowing argon in order to allow the iridium to

preferentially react with oxygen from the ruthenium oxide, and not oxygen from the environment.

Nanoparticulate iridium black and anhydrous ruthenium oxide are weighed out and mixed to 5–18 atomic percent. They are then heat treated at 300 °C under flowing argon (in order to create an inert environment) for a minimum of 14 hours. This temperature was chosen because it is approximately the creep temperature of ruthenium oxide, and is below the sintering temperature of both materials. In general, the temperature should always be below the sintering temperature of both materials. The iridium-doped ruthenium oxide catalyst is

then fabricated into a PEM-based membrane-electrode assembly (MEA), and then mounted into test cells.

The result is an electrolyzer system that can sustain electrolysis at twice the current density, and at the same efficiency as commercial catalysts in the range of 100–200 mA/cm². At 200 mA/cm², this new system operates at an efficiency of 85 percent, which is 2 percent greater than commercially available catalysts. Testing has shown that this material is as stable as commercially available oxygen evolution catalysts. This means that this new catalyst can be used to regenerate fuel cell systems in space, and as a hydrogen generator on Earth.

This work was done by Thomas I. Valdez, Sri R. Narayan, and Keith J. Billings of Caltech for NASA's Jet Propulsion Laboratory. Further information is contained in a TSP (see page 1).

In accordance with Public Law 96-517, the contractor has elected to retain title to this invention. Inquiries concerning rights for its commercial use should be addressed to:

*Innovative Technology Assets Management
JPL*

*Mail Stop 202-233
4800 Oak Grove Drive
Pasadena, CA 91109-8099*

E-mail: iaoffice@jpl.nasa.gov

Refer to NPO-46387, volume and number of this NASA Tech Briefs issue, and the page number.

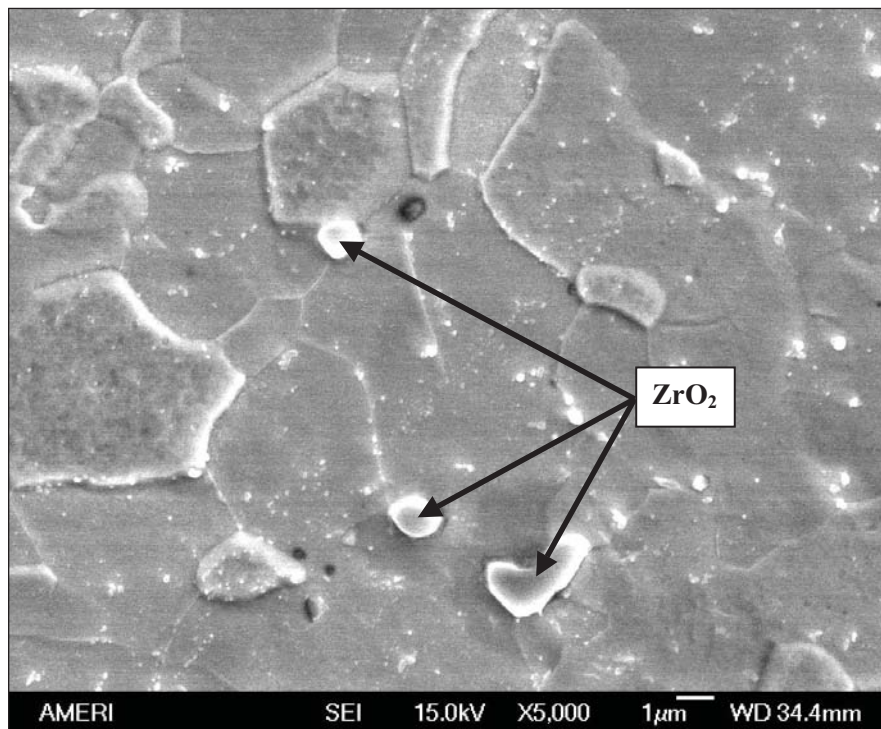
Improved Mo-Re VPS Alloys for High-Temperature Uses

Transition-metal ceramic dispersoids improve high-temperature properties.

Marshall Space Flight Center, Alabama

Dispersion-strengthened molybdenum-rhenium alloys for vacuum plasma spraying (VPS) fabrication of high-temperature-resistant components are undergoing development. In comparison with otherwise equivalent non-dispersion-strengthened Mo-Re alloys, these alloys have improved high-temperature properties. Examples of VPS-fabricated high-temperature-resistant components for which these alloys are expected to be suitable include parts of aircraft and spacecraft engines, furnaces, and nuclear power plants; wear coatings; sputtering targets; x-ray targets; heat pipes in which liquid metals are used as working fluids; and heat exchangers in general. These alloys could also be useful as coating materials in some biomedical applications.

The alloys consist of 60 weight percent Mo with 40 weight percent Re made from (1) blends of elemental Mo and Re powders or (2) Re-coated Mo particles that have been subjected to a proprietary powder-alloying-and-spheroidization process. For most of the dispersion-strengthening experiments performed thus far in this development effort, 0.4 volume percent of transition-metal ceramic dispersoids were mixed into the feedstock powders. For one experiment, the proportion of dispersoid was 1 volume percent. In each case, the dispersoid consisted of either ZrN particles having sizes <45 μm, ZrO₂ particles having sizes of about 1 μm, HfO₂ parti-



This Scanning Electron Micrograph of a dispersion-strengthened specimen shows ZrO₂ particles at grain boundaries of the Mo-Re alloy.

cles having sizes <45 μm, or HfN particles having sizes <1 μm. These materials were chosen for evaluation on the basis of previously published thermodynamic stability data. For comparison, Mo-Re feedstock powders without dispersoids were also prepared.

Tubular alloy specimens were fabricated by VPS onto rotating graphite

mandrels as follows: In each case, the VPS chamber was evacuated, then the rotating graphite mandrel was preheated by the plasma spray gun. Once the desired preheat temperature was reached, one of the powders prepared as described above was made to flow to the gun, causing the alloy to be deposited on the mandrel. [A nearly iden-

tical process for fabrication of tubes of non-dispersion-strengthened Mo-Re tubes was described in "High-Temperature Crystal-Growth Cartridge Tubes Made by VPS" (MFS-31540), *NASA Tech Briefs*, Vol. 32, No. 11 (November 2008, page 54).] Immediately after VPS and before removal from the VPS chamber, the deposit and mandrel were cooled under a partial pressure of argon. After removal from the chamber, the mandrel was mechanically removed, leaving the tubular specimen.

The specimens were subjected to aging/grain-growth tests and to both room-temperature and elevated-temperature tensile tests. The conclusions drawn from the test results include the following:

- It is possible, by use of VPS, to fabricate Mo-Re alloys of the type in question to

nearly net size and shape, having densities greater than 97 percent of the theoretical maximum.

- Microscopic examination of samples that had been aged at a temperature of 1,800 °C for 8 hours showed that average grain sizes in the samples containing dispersoids were significantly less than those of the samples that did not contain dispersoids. This result was interpreted as signifying that the dispersoids pinned Mo-Re grain boundaries (see figure) and thereby reduced grain growth.
- Room- and elevated-temperature tensile tests of two of the dispersion-strengthened alloys and of the corresponding nondispersion-strengthened alloys showed that dispersion strengthening afforded significant improvements in mechanical properties:
 - Dispersion strengthening did not

cause a decrease in room-temperature elongation.

- The elevated-temperature ultimate tensile strengths of the dispersion-strengthened alloys were between 16 and 18 percent greater than those of the non-dispersion-strengthened alloys.
- The room-temperature mechanical properties of the dispersion-strengthened alloys equaled or exceeded previously published values for alloys comprising 60 weight percent of Mo with 40 weight percent of Re.

This work was done by Robert Hickman and James Martin of Marshall Space Flight Center and Timothy McKechnie and John (Scott) O'Dell of Plasma Processes, Inc. For further information, contact Sammy Nabors, MSFC Commercialization Assistance Lead, at sammy.a.nabors@nasa.gov. Refer to MFS-32581-1.



Data Service Provider Cost Estimation Tool

Goddard Space Flight Center, Greenbelt, Maryland

The Data Service Provider Cost Estimation Tool (CET) and Comparables Database (CDB) package provides to NASA's Earth Science Enterprise (ESE) the ability to estimate the full range of year-by-year lifecycle cost estimates for the implementation and operation of data service providers required by ESE to support its science and applications programs. The CET can make estimates dealing with staffing costs, supplies, facility costs, network services, hardware and maintenance, commercial off-the-shelf (COTS) software licenses, software de-

velopment and sustaining engineering, and the changes in costs that result from changes in workload.

Data Service Providers may be stand-alone or embedded in flight projects, field campaigns, research or applications projects, or other activities. The CET and CDB package employs a cost-estimation-by-analogy approach. It is based on a new, general data service provider reference model that provides a framework for construction of a database by describing existing data service providers that are analogs (or compara-

bles) to planned, new ESE data service providers. The CET implements the staff effort and cost estimation algorithms that access the CDB and generates the lifecycle cost estimate for a new data services provider. This data creates a common basis for an ESE proposal evaluator for considering projected data service provider costs.

This program was written by Kathy Fontaine of Goddard Space Flight Center and Greg Hunolt, Arthur L. Booth, and Mel Banks of SGT, Inc. Further information is contained in a TSP (see page 1). GSC-14905-1

Hybrid Power Management-Based Vehicle Architecture

This ultracapacitor design is energy- and cost-efficient with measurably less environmental impact.

John H. Glenn Research Center, Cleveland, Ohio

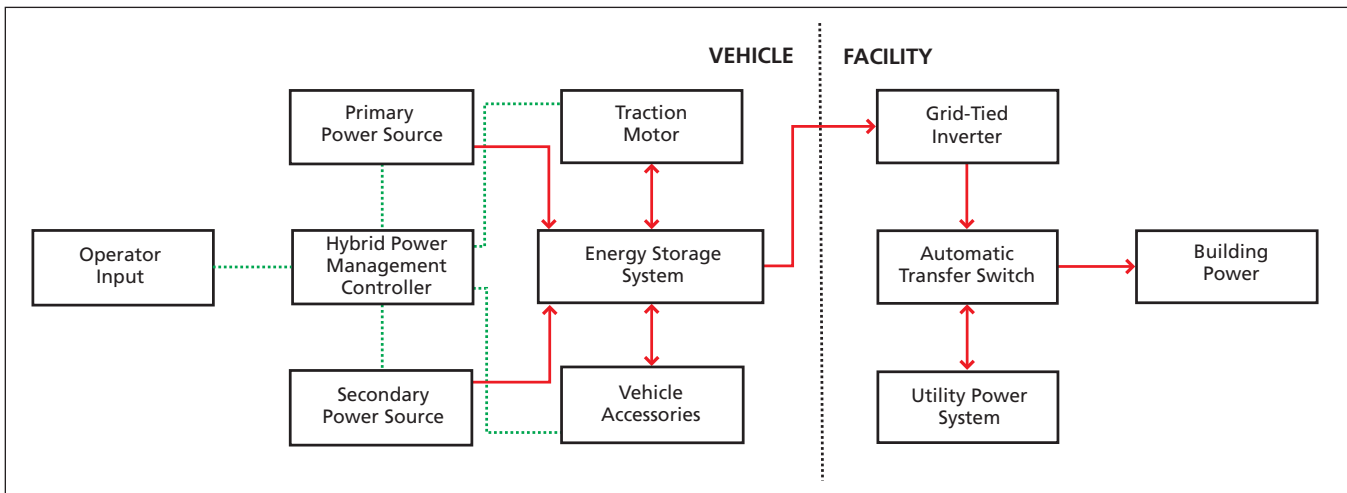
Hybrid Power Management (HPM) is the integration of diverse, state-of-the-art power devices in an optimal configuration for space and terrestrial applications (see figure). The appropriate application and control of the various power devices significantly improves overall system performance and efficiency. The basic vehicle architecture consists of a primary power source, and possibly other power sources, that pro-

vides all power to a common energy storage system that is used to power the drive motors and vehicle accessory systems. This architecture also provides power as an emergency power system.

Each component is independent, permitting it to be optimized for its intended purpose. The key element of HPM is the energy storage system. All generated power is sent to the energy storage system, and all loads derive their

power from that system. This can significantly reduce the power requirement of the primary power source, while increasing the vehicle reliability.

Ultracapacitors are ideal for an HPM-based energy storage system due to their exceptionally long cycle life, high reliability, high efficiency, high power density, and excellent low-temperature performance. Multiple power sources and multiple loads are easily



General HPM Vehicle Architecture.

incorporated into an HPM-based vehicle. A gas turbine is a good primary power source because of its high efficiency, high power density, long life, high reliability, and ability to operate on a wide range of fuels. An HPM controller maintains optimal control over each vehicle component. This flexible operating system can be applied to all vehicles to considerably improve vehicle efficiency, reliability, safety, security, and performance.

The HPM-based vehicle architecture has many advantages over conventional vehicle architectures. Ultracapacitors

have a much longer cycle life than batteries, which greatly improves system reliability, reduces life-of-system costs, and reduces environmental impact as ultracapacitors will probably never need to be replaced and disposed of. The environmentally safe ultracapacitor components reduce disposal concerns, and their recyclable nature reduces the environmental impact. High ultracapacitor power density provides high power during surges, and the ability to absorb high power during recharging. Ultracapacitors are extremely efficient in capturing recharging energy, are rugged, reliable,

maintenance-free, have excellent low-temperature characteristic, provide consistent performance over time, and promote safety as they can be left indefinitely in a safe, discharged state whereas batteries cannot.

This work was done by Dennis J. Eichenberg of Glenn Research Center. Further information is contained in a TSP (see page 1).

Inquiries concerning rights for the commercial use of this invention should be addressed to NASA Glenn Research Center, Innovative Partnerships Office, Attn: Steven Fedor, Mail Stop 4-8, 21000 Brookpark Road, Cleveland, Ohio 44135. Refer to LEW-18704-1.



Force Limit System

This system protects the operator, specimen, system, and fixtures from overload damage.

John H. Glenn Research Center, Cleveland, Ohio

The Force Limit System (FLS) was developed to protect test specimens from inadvertent overload. The load limit value is fully adjustable by the operator and works independently of the test system control as a mechanical (non-electrical) device.

When a test specimen is loaded via an electromechanical or hydraulic test system, a chance of an overload condition exists. An overload applied to a specimen could result in irreparable damage to the specimen and/or fixturing. The FLS restricts the maximum load that an actuator can apply to a test specimen. When testing limited-run test articles or using very expensive fixtures, the use of such a device is highly recommended. Test setups typically use electronic peak protection, which can be the source of overload due to malfunctioning components or the inability to react quickly enough to load spikes. The FLS works independently of the electronic overload protection.

In a standard test system, an actuator moves in a uniaxial direction to apply load to a fixed-position specimen in a very controlled fashion. The actuator, usually capable of very high loads, is normally driven by an electromechanical motor or hydraulic power supply. So-

phisticated electronic/software packages command the movement of the actuator based on transducer input and operator requirements. This is all independent of the FLS.

The Force Limit Cylinder is preset to a calibrated amount that equals the safety factor or protection value desired by the operator. The maximum force is determined by a precision dynamic mechanical control that has a very high relief rate. The load values and relief rates are dictated by test requirements. The Force Limit Cylinder is attached to the actuator on one end, and test specimen contact on the other end (usually the cylinder push rod). Standard fixture alignment procedures should be used prior to specimen loading.

Before applying load to the specimen, the Force Limit Cylinder should be preset to the desired value to equal the desired load limit. Once this is completed, the Force Limit Cylinder push rod will not permit the actuator to exceed the preset load to the specimen. If the actuator increases load to the point of the FLS set point, the Force Limit Cylinder push rod will retract as the mechanical control relieves force. If the actuator continues to move downward, the Force Limit Cylinder will allow this until the

actuator contacts its internal mechanical stops.

The unique features of this device are that it has an independent, fully adjustable load limit using mechanical design, and it has the ability to change test frame control channels with minimal risk by applying load while in position control. For simplicity, the FLS uses readily available parts.

The FLS can also be used in a test system that has no provision for control mode switching to an advantage. When a test system is switched between position control and load control, there is an increased risk of overload during this operation. The FLS can be used to apply a very low load to a specimen while controlled in position. This allows a safe control mode switch and avoids an open-loop situation.

This work was done by Ralph Pawlik, David Krause, and Frank Bremenour of Glenn Research Center. Further information is contained in a TSP (see page 1).

Inquiries concerning rights for the commercial use of this invention should be addressed to NASA Glenn Research Center, Innovative Partnerships Office, Attn: Steven Fedor, Mail Stop 4-8, 21000 Brookpark Road, Cleveland, Ohio 44135. Refer to LEW-18678-1.

Levitated Duct Fan (LDF) Aircraft Auxiliary Generator

This all-electric design eliminates mechanical bearings and enables more efficient aircraft electrical systems.

John H. Glenn Research Center, Cleveland, Ohio

This generator concept includes a novel stator and rotor architecture made from composite material with blades attached to the outer rotating shell of a ducted fan drum rotor, a non-contact support system between the stator and rotor using magnetic fields to provide levitation, and an integrated electromagnetic generation system. The magnetic suspension be-

tween the rotor and the stator suspends and supports the rotor within the stator housing using permanent magnets attached to the outer circumference of the drum rotor and passive levitation coils in the stator shell. The magnets are arranged in a Halbach array configuration.

The electromagnetic generation system also uses permanent magnets at-

tached to the outer circumference of the drum rotor with coils placed in the stator shell. The generation system uses the same magnets as the levitation system, but incorporates generator coils in the stator that are interwoven with passive levitation coils. The levitation system is inherently stable, is failsafe, and does not require active control as required by traditional magnetic bear-

ings. Also, the overall efficiency of the suspension system improves with speed, whereas the performance of conventional bearings degrades as speed increases.

This innovation will greatly advance aircraft electrical power systems with the development of an efficient, reliable, maintenance-free, and safe electrical generation system. The use of magnetic suspension minimizes concerns associated with traditional bearings, such as active lubrication, contact wear, and limited rotational speed. The ducted hardware can translate into improved efficiency and reliability. The concept lends itself to a configuration in which the units can be used individually or clustered for distributed power applications. In addition, the concept can be readily scaled into a variety of sizes for specified

power delivery with similar geometric configuration. The rotor operates in compression, which results in a 2× improvement in fatigue life, and the extensive use of composites minimizes weight and reduces noise due to the higher dampening properties of composites.

A prototype stator and assembly and rotor have been designed and developed to study and evaluate subsystem level characteristics of the generation and levitation systems in a laboratory environment, and to verify theoretical predictions. The test setup has been used to measure successfully the flux density emanating from the rotor, the induced current in the stator winding as the rotor is driven at various speeds, the associated induced current, and the generated repulsive force. Experimental results correlate well with per-

formance characteristics predicted using the derived theoretical equations. The goal of the final design is a self-contained suspension and electrical generation system free from mechanical couplings. The use of magnetic suspension minimizes concerns associated with traditional bearings, such as active lubrication and limited rotational speeds.

This work was done by Dennis J. Eichenberg, Dawn C. Emerson, Christopher A. Gallo, and William K. Thompson of Glenn Research Center. Further information is contained in a TSP (see page 1).

Inquiries concerning rights for the commercial use of this invention should be addressed to NASA Glenn Research Center, Innovative Partnerships Office, Attn: Steven Fedor, Mail Stop 4-8, 21000 Brookpark Road, Cleveland, Ohio 44135. Refer to LEW-18658-1.

⚙️ Compact, Two-Sided Structural Cold Plate Configuration

Lyndon B. Johnson Space Center, Houston, Texas

In two-sided structural cold plates, typically there is a structural member, such as a honeycomb panel, that provides the structural strength for the cold plates that cool equipment. The cold plates are located on either side of the structural member and thus need to have the cooling fluid supplied to them. One method of accomplishing this is to route the inlet and outlet tubing to both sides of the structural member. Another method might be to supply the inlet to one side and the outlet to the other. With the latter method, an external feature such as a hose, tube, or manifold must be incorporated to pass the fluid from one side of the structural member to the other. Although this is a more compact design than the first option, since it eliminates the need for a dedicated supply and return line to each side of the structural member, it still poses problems, as these

external features can be easily damaged and are now new areas for potential fluid leakage.

This invention eliminates the need for an external feature and instead incorporates the feature internally to the structural member. This is accomplished by utilizing a threaded insert that not only connects the cold plate to the structural member, but also allows the cooling fluid to flow through it into the structural member, and then to the cold plate on the opposite side. The insert also employs a cap that acts as a cover to seal the open area needed to install the insert. There are multiple options for location of o-ring style seals, as well as the option to use adhesive for redundant sealing. Another option is to weld the cap to the cold plate after its installation, thus making it an integral part of the structural member. This new

configuration allows the fluid to pass from one cold plate to the other without any exposed external features.

This work was done by Mark Zaffetti of Hamilton Sundstrand for Johnson Space Center. For further information, contact the JSC Innovation Partnerships Office at (281) 483-3809.

Title to this invention has been waived under the provisions of the National Aeronautics and Space Act {42 U.S.C. 2457(f)} to Hamilton Sundstrand. Inquiries concerning licenses for its commercial development should be addressed to:

*Hamilton Sundstrand
Space Systems International, Inc.
One Hamilton Road
Windsor Locks, CT 06096-1010
Phone No.: (860) 654-6000*

Refer to MSC-24880-1, volume and number of this NASA Tech Briefs issue, and the page number.

⚙️ AN Fitting Reconditioning Tool

John F. Kennedy Space Center, Florida

A tool was developed to repair or replace AN fittings on the shuttle external tank (ET). (The AN thread is a type of fitting used to connect flexible hoses and rigid metal tubing that carry fluid. It is a U.S. military-derived specifica-

tion agreed upon by the Army and Navy, hence AN.) The tool is used on a drill and is guided by a pilot shaft that follows the inside bore. The cutting edge of the tool is a standard-size replaceable insert. In the typical Post

Launch Maintenance/Repair process for the AN fittings, the six fittings are removed from the ET's GUCP (ground umbilical carrier plate) for reconditioning. The fittings are inspected for damage to the sealing surface per stan-

standard operations maintenance instructions. When damage is found on the sealing surface, the condition is documented.

A new AN reconditioning tool is set up to cut and remove the surface damage. It is then inspected to verify the fitting still meets drawing requirements. The tool features a cone-shaped interior

at 36.5°, and may be adjusted at a precise angle with go-no-go gauges to insure that the cutting edge could be adjusted as it wore down. One tool, one setting block, and one go-no-go gauge were fabricated. At the time of this reporting, the tool has reconditioned/returned to spec 36 AN fittings with 100-percent success of no leakage.

This tool provides a quick solution to repair a leaky AN fitting. The tool could easily be modified with different-sized pilot shafts to different-sized fittings.

This work was done by Jason Lopez of Kennedy Space Center. Further information is contained in a TSP (see page 1). KSC-13235

Active Response Gravity Offload System

Lyndon B. Johnson Space Center, Houston, Texas

The Active Response Gravity Offload System (ARGOS) provides the ability to simulate with one system the gravity effect of planets, moons, comets, asteroids, and microgravity, where the gravity is less than Earth's gravity. The system works by providing a constant force of float through an overhead hoist system and horizontal motion through a rail and trolley system. The facility covers a 20- by 40-ft (≈6.1- by 12.2-m) horizontal area with 15 ft (≈4.6 m) of lifting vertical range.

The overall design and implementation of the ARGOS system is unique and is at the time of this reporting the only known system of its kind. The interface of ARGOS to the human test participant is critical and is provided by a gimbaled system that was developed to align the pitch, yaw, and roll axes, and offload force provided by ARGOS, with the center of gravity of the object or person being lifted. This gimbaled system greatly improves the realistic feel of the simulated gravity to the person in the

simulation. Therefore, the system allows the person to perform tasks such as walking as if the individual was on the surface of the celestial body being simulated. The system has been used for bipedal walking robots and human testing in a variety of simulated gravitation fields.

This work was done by Paul Valle, Larry Dungan, Thomas Cunningham, Asher Lieberman, and Dina Poncia of Johnson Space Center. Further information is contained in a TSP (see page 1). MSC-24815-1/24-1



Method and Apparatus for Forming Nanodroplets

This technique can create functionalized particles for targeted drug delivery.

Lyndon B. Johnson Space Center, Houston, Texas

This innovation uses partially miscible fluids to form nano- and micro-droplets in a microfluidic droplet generator system.

Droplet generators fabricated in PDMS (polydimethylsiloxane) are currently being used to fabricate engineered nanoparticles and microparticles. These droplet generators were first demonstrated in a T-junction configuration, followed by a cross-flow configuration. All of these generating devices have used immiscible fluids, such as oil and water. This immiscible fluid system can produce mono-dispersed distributions of droplets and articles with sizes ranging from a few hundred nanometers to a few hundred microns. For applications such as drug delivery, the ability to encapsulate aqueous solutions of drugs within particles formed from the droplets is desirable.

Of particular interest are non-polar solvents that can dissolve lipids for the formation of liposomes in the droplet generators. Such fluids include ether, cyclohexane, butanol, and ethyl acetate. Ethyl acetate is of particular interest for two reasons. It is relatively non-toxic and it is formed from ether and acetic acid, and maybe broken down into its constituents at relatively low concentrations.

Further investigation of the liposome properties reveals that optimal liposome-forming mixtures have sufficient density and viscosity to form droplets, but also have the potential to be exchanged from aqueous solutions. Overall, ethyl acetate was found to be about 8 percent miscible in water, which suggests that it could eventually be exchanged into a buffer solution. Based on this solubility for ethyl acetate in water, it was hypothesized that this mixture of reagents was sufficiently immiscible to form droplets on the device. Also, the PDMS droplet generator devices were sufficiently resistant to the solvent effects of ethyl acetate and remained stable during the liposome-forming process.

The fluidic system looks very much like other solvent/water systems. Droplets in the range of 100 to 5,000 nm in diameter may be formed by adjusting the flow rates. Liposomes were successfully fabricated in the ethyl acetate/water system using various lipid mixtures. The liposomes were formed by dissolving a lipid mixture in ethyl acetate, and producing droplets, in the droplet generator. After droplet formation, the droplets flowed from an outlet and were dried down in a collection tube. This demonstrated the advantage of the

droplet fluid system when the solvent phase has a high vapor pressure. After dry-down, the liposomes could then be rehydrated into an aqueous (buffer) solution for further use.

By way of contrast, a major limitation to the immiscible fluid system is the fact that the nanodroplets form an oil/water emulsion when aqueous droplets are formed in oil. In the case of nano- and micro-particle formation from the droplets, it is very difficult to separate out the target particles from the oil in the emulsion. Thus, it was desirable to demonstrate an alternative solvent system from which the particles can be more readily separated.

This work was done by Donald Ackley and Anita Forster of Nanotrope Inc. for Johnson Space Center. For further information, contact the JSC Innovation Partnerships Office at (281) 483-3809.

In accordance with Public Law 96-517, the contractor has elected to retain title to this invention. Inquiries concerning rights for its commercial use should be addressed to:

Nanotrope Inc.

2033 Cambridge Ave.

Cardiff, CA 92007

Phone No.: (760) 942-0301

Refer to MSC-24082-1, volume and number of this NASA Tech Briefs issue, and the page number.

Rapid Detection of the *Varicella Zoster Virus* in Saliva

This kit provides a rapid, sensitive, specific, and inexpensive method for early virus detection.

Lyndon B. Johnson Space Center, Houston, Texas

Varicella zoster virus (VZV) causes chicken pox on first exposure (usually in children), and reactivates from latency causing shingles (usually in adults). Shingles can be extremely painful, causing nerve damage, organ damage, and blindness in some cases. The virus can be life-threatening in immune-compromised individuals. The virus is very difficult to culture for diagnosis, requiring a week or longer.

This invention is a rapid test for VZV from a saliva sample and can be performed in a doctor's office. The kit is small, compact, and lightweight. Detection is sensitive, specific, and noninvasive (no needles); only a saliva sample is required. The test provides results in minutes. The entire test is performed in a closed system, with no exposure to infectious materials. The components are made mostly of inex-

pensive plastic injection molded parts, many of which can be purchased off the shelf and merely assembled. All biological waste is contained for fast, efficient disposal.

This innovation was made possible because of discovery of a NASA scientists' flight experiment showing the presence of VZV in saliva during high stress periods and disease. This finding enables clinicians to quickly screen patients for

VZV and treat the ones that show positive results with antiviral medicines. This promotes a rapid recovery, easing of pain and symptoms, and reduces chances of complications from zoster.

Screening of high-risk patients could be incorporated as part of a regular physical exam. These patients include the elderly, pregnant women,

and immune-compromised individuals. In these patients, VZV can be a life-threatening disease. In both high- and low-risk patients, early detection and treatment with antiviral drugs can dramatically decrease or even eliminate the clinical manifestation of disease.

This work was done by Duane L. Pierson of Johnson Space Center; Satish K. Mehta of

EASI; Randall J. Cohrs and Don H. Gilden of the University of Colorado Health Science Center; and Robert E. Harding, independent consultant. Inquiries concerning rights for the commercial use of this invention should be addressed to David Poticha at the University of Colorado, david.poticha@cu.edu. Refer to MSC-24451-1.

Improved Devices for Collecting Sweat for Chemical Analysis

Unlike prior devices, these would enable measurement of volumes of specimens.

Lyndon B. Johnson Space Center, Houston, TX

Improved devices have been proposed for collecting sweat for biochemical analysis — especially for determination of the concentration of Ca^{2+} ions in sweat as a measure of loss of Ca from bones. Unlike commercially available sweat-collection patches used previously in monitoring osteoporosis and in qualitative screening for some drugs, the proposed devices would not allow evaporation of the volatile chemical components (mostly water) of sweat. Moreover, the proposed devices would be designed to enable determination of the volumes of collected sweat. From these volumes and the quantities of Ca^{2+} and/or other analytes as determined by other means summarized below, one could determine the concentrations of the analytes in sweat.

A device according to the proposal would be flexible and would be worn like a commercial sweat-collection patch. It would be made of molded poly-

dimethylsiloxane (silicone rubber) or other suitable material having properties that, for the purpose of analyzing sweat, are similar to those of glass. The die for molding the silicone rubber would be fabricated by a combination of lithography and electroplating. The die would reproducibly form, in the silicone rubber, a precisely defined number of capillary channels per unit area, each channel having a precisely defined volume. Optionally, electrodes for measuring the Ca^{2+} content of the sweat could be incorporated into the device.

The volume of sweat collected in the capillary channels of the device would be determined from (1) the amount of light or radio waves of a given wavelength absorbed by the device and (2) the known geometry of the array of capillary channels. Then, in one of two options, centrifugation would be performed to move the sweat from the capillary tubes to the region containing

the electrodes, which would be used to measure the Ca^{2+} content by a standard technique. In the other option, centrifugation would be performed to remove the sweat from the device to make the sweat available to other analytical instruments for measuring concentrations of substances other than Ca^{2+} .

This work was done by Daniel L. Feeback of Johnson Space Center and Mark S. F. Clarke of the University of Houston. Further information is contained in a TSP (see page 1).

In accordance with Public Law 96-517, the contractor has elected to retain title to this invention. Inquiries concerning rights for its commercial use should be addressed to:

*University of Houston
Department of Health and Human Performance
Laboratory of Integrated Physiology
3855 Holman St., Room 104 Garrison
Houston, TX 77201*

Refer to MSC-23625-1, volume and number of this Medical Design Briefs issue, and the page number.



Phase-Controlled Magnetic Mirror for Wavefront Correction

Goddard Space Flight Center, Greenbelt, Maryland

Typically, light interacts with matter via the electric field and interaction with weakly bound electrons. In a magnetic mirror, a patterned nanowire is fabricated over a metallic layer with a dielectric layer in between. Oscillation of the electrons in the nanowires in response to the magnetic field of incident photons causes a re-emission of photons and operation as a “magnetic mirror.” By controlling the index of refraction in the dielectric layer using a local applied voltage, the phase of the emitted radiation can be controlled. This allows electrical modification of the reflected wavefront, resulting in a deformable mirror that can be used for wavefront control.

Certain applications require wavefront quality in the few-nanometer regime, which is a major challenge for optical fabrication and alignment of

mirrors or lenses. The use of a deformable magnetic mirror allows for a device with no moving parts that can modify the phase of incident light over many spatial scales, potentially with higher resolution than current approaches. Current deformable mirrors modify the incident wavefront by using nano-actuation of a substrate to physically bend the mirror to a desired shape.

The purpose of the innovation is to modify the incident wavefront for the purpose of correction of fabrication and alignment-induced wavefront errors at the system level. The advanced degree of precision required for some applications such as gravity wave detection (LISA — Laser Interferometer Space Antenna) or planet finding (FKSI — Fourier-Kelvin Stellar Interferometer) requires wavefront control at the limits of the current state of the art.

All the steps required to fabricate a magnetic mirror have been demonstrated. The modification is to apply a bias voltage to the dielectric layer so as to change the index of refraction and modify the phase of the reflected radiation. Light is reflected off the device and collected by a phase-sensing interferometer. The interferometer determines the initial wavefront of the device and fore optics. A wavefront correction is calculated, and voltage profile for each nanowire strip is determined. The voltage is applied, modifying the local index of refraction of the dielectric under the nanowire strip. This modifies the phase of the reflected light to allow wavefront correction.

This work was done by John Hagopian and Edward Wollack of Goddard Space Flight Center. Further information is contained in a TSP (see page 1). GSC-16008-1

Frame-Transfer Gating Raman Spectroscopy for Time-Resolved Multiscalar Combustion Diagnostics

This invention could potentially benefit the development of advanced combustion systems such as gas turbine engines and internal combustion engines.

John H. Glenn Research Center, Cleveland, Ohio

Accurate experimental measurement of spatially and temporally resolved variations in chemical composition (species concentrations) and temperature in turbulent flames is vital for characterizing the complex phenomena occurring in most practical combustion systems. These diagnostic measurements are called multiscalar because they are capable of acquiring multiple scalar quantities simultaneously. Multiscalar diagnostics also play a critical role in the area of computational code validation. In order to improve the design of combustion devices, computational codes for modeling turbulent combustion are often used to speed up and optimize the development process. The experimental validation of these codes is a critical step in accepting their predictions for engine performance in

the absence of cost-prohibitive testing.

One of the most critical aspects of setting up a time-resolved stimulated Raman scattering (SRS) diagnostic system is the temporal optical gating scheme. A short optical gate is necessary in order for weak SRS signals to be detected with a good signal-to-noise ratio (SNR) in the presence of strong background optical emissions. This time-synchronized optical gating is a classical problem even to other spectroscopic techniques such as laser-induced fluorescence (LIF) or laser-induced breakdown spectroscopy (LIBS). Traditionally, experimenters have had basically two options for gating: (1) an electronic means of gating using an image intensifier before the charge-coupled-device (CCD), or (2) a mechanical optical shutter (a rotary chopper/mechanical shutter combination).

A new diagnostic technology has been developed at the NASA Glenn Research Center that utilizes a frame-transfer CCD sensor, in conjunction with a pulsed laser and multiplex optical fiber collection, to realize time-resolved Raman spectroscopy of turbulent flames that is free from optical background noise (interference). The technology permits not only shorter temporal optical gating (down to $<1 \mu\text{s}$, in principle), but also higher optical throughput, thus resulting in a substantial increase in measurement SNR.

The new technology is an experimental method (or scheme) for isolating true Raman spectral signals from flames using a single CCD detector. It does not use an image intensifier or a mechanical shutter. Individual electrical or optical devices employed in this method are not

new; however, the diagnostic methodology itself, which utilizes a combination of existing devices for a particular application, is a novel concept.

The present methodology employs two key optical devices: a pulsed laser (nanosecond pulses) and a frame-transfer CCD sensor. Frame-transfer CCD sensors have been historically used to capture fast (microsecond timescale) transient events, such as Bose-Einstein condensate phenomena, over a short period of time (milliseconds). By their operation, the sensor area is exposed for a certain time and the charge is then transferred to the frame transfer area (or masking area) row-by-row, and is read out via a gain register or serial register. This is called "frame-transfer" readout or "kinetics" readout. The use of frame-transfer readout provides a very

effective way of isolating true Raman signals from laser-generated optical interferences in any combustion environment, in principle, without having to employ multiple CCD detectors or polarizer on the detection side.

Since laser-induced background emissions are unpolarized, unlike Raman scattering, which is polarized, they can be selectively isolated (and subtracted). While the theory of this polarization technique has been proposed previously, the implementation of this technique for time-resolved Raman diagnostics has not been matured. A principal reason is that an enabling technology that can increase the SNR was needed. When a flame receives two orthogonally polarized, but otherwise identical, laser pulses, Raman scattering can be observable only for the vertically polarized excitation pulse. The

(unpolarized) laser-generated background emissions are observed regardless of the polarization state of the excitation pulses. If the two orthogonally-polarized laser pulses are separated in time so that they just fall onto a pair of consecutive sub-frames on the CCD sensor, subtracting the one (laser-generated background emission only) from the other (Raman signal plus background emission) results in a true Raman spectrum.

This work was done by Quang-Viet Nguyen, David G. Fischer, and Jun Kojima of Glenn Research Center. Further information is contained in a TSP (see page 1).

Inquiries concerning rights for the commercial use of this invention should be addressed to NASA Glenn Research Center, Innovative Partnerships Office, Attn: Steven Fedor, Mail Stop 4-8, 21000 Brookpark Road, Cleveland, Ohio 44135. Refer to LEW-18483-1.

Thermal Properties of Microstrain Gauges Used for Protection of Lithium-Ion Cells of Different Designs

Commercial uses include lithium-ion batteries used in a human-rated environment, such as in automobile applications.

Lyndon B. Johnson Space Center, Houston, Texas

The purpose of this innovation is to use microstrain gauges to monitor minute changes in temperature along with material properties of the metal cans and pouches used in the construction of lithium-ion cells. The sensitivity of the microstrain gauges to extremely small changes in temperatures internal to the cells makes them a valuable asset in controlling the hazards in lithium-ion cells. The test program on lithium-ion cells included various cell configurations, including the pouch type configurations.

The thermal properties of microstrain gauges have been found to contribute significantly as safety monitors in lithium-ion cells that are designed even with hard metal cases. Although the metal cans do not undergo changes in material property, even under worst-case unsafe conditions, the small changes in thermal properties observed during charge and discharge of the cell provide an observable change in resistance of the strain gauge. Under abusive or unsafe conditions, the change in the resistance is large. This large change is observed as a significant change in slope, and this can be used to prevent cells from going into a thermal runaway condition. For flexible metal cans or

pouch-type lithium-ion cells, combinations of changes in material properties along with thermal changes can be used as an indication for the initiation of an unsafe condition.

Lithium-ion cells have a very high energy density, no memory effect, and almost 100-percent efficiency of charge and discharge. However, due to the presence of a flammable electrolyte, along with the very high energy density and the capability of releasing oxygen from the cathode, these cells can go into a hazardous condition of venting, fire, and thermal runaway. Commercial lithium-ion cells have current and voltage monitoring devices that are used to control the charge and discharge of the batteries. Some lithium-ion cells have internal protective devices, but when used in multi-cell configurations, these protective devices either do not protect or are themselves a hazard to the cell due to their limitations. These devices do not help in cases where the cells develop high impedance that suddenly causes them to go into a thermal runaway condition. Temperature monitoring typically helps with tracking the performance of a battery. But normal thermistors or thermal sensors do not

provide the accuracy needed for this and cannot track a change in internal cell temperatures until it is too late to stop a thermal runaway.

The microstrain gauges under study have shown remarkable changes in resistance with changes in temperature that show a very close tracking to the current used to charge and discharge the lithium-ion cells. As the cells are charged, there is a very slight increase in temperature at the end of charge, and the same during the discharge process. Although normal thermistors do not show a big change in temperature, the strain gauges have been able to track with great accuracy the thermal changes in the cells during these processes. Although strain gauges have been used to track pressures internal to cells in battery chemistries that use pressure vessels such as the Ni-hydrogen cells, they have not been used to track resistance changes due to temperatures. Existing thermal sensors do not have the sensitivity to be able to track small changes in internal temperatures of the cells, so monitoring systems cannot detect changes fast enough to be able to provide any protection. With lithium-ion cells, when the thermal sensors

record an alarming temperature reading, it indicates that the cell's internal temperatures have reached a point where no external controls can stop the thermal runaway. With the thermally sensitive new strain gauges, the changes in slope are so sensitive that this change can be used to stop the charge or remove the load on the lithium-ion cells before the event can spiral into an uncontrollable one.

Four different configurations of lithium-ion cells were tested. Two cylindrical cells with metal containers (two different diameters), a prismatic metal container cell type, and a pouch cell type (aluminized plastic pouch) were used for the study. Several tests were performed on all our designs. The tests included normal charge and discharge cycling at two different charge and discharge rates at room temperature and at

low temperature. The tests also included off-nominal conditions of overcharge, overdischarge, external short, heat-to-vent, and crush (simulated internal short). Overcharge tests and external short tests provide the most valuable data as these conditions produce the worst-case reactions in lithium-ion cells.

This work was done by Judith Jeevarajan of Johnson Space Center. Further information is contained in a TSP (see page 1). MSC-24764-1

In-Service Monitoring of Steam Pipe Systems at High Temperatures

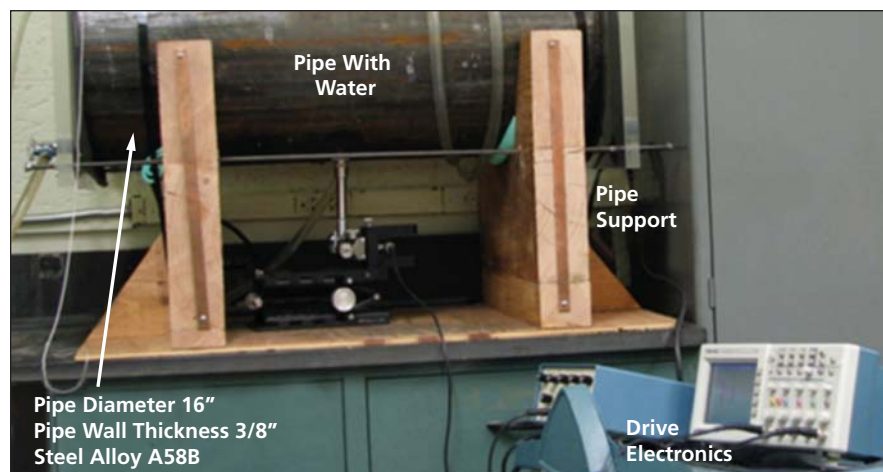
This system can be used by utility companies for steam pipe systems incorporating multiple manholes.

NASA's Jet Propulsion Laboratory, Pasadena, California

An effective, in-service health monitoring system is needed to track water condensation in real time through the walls of steam pipes. The system is required to measure the height of the condensed water from outside the pipe, while operating at temperatures that are as high as 250 °C. The system needs to account for the effects of water flow and cavitation. In addition, it is desired that the system does not require perforating the pipes and thereby reducing the structural integrity.

Generally, steam pipes are used as part of the district heating system carrying steam from central power stations under the streets to heat, cool, or supply power to high-rise buildings and businesses. This system uses ultrasonic waves in pulse-echo and acquires reflected signal data. Via autocorrelation, it determines the water height while eliminating the effect of noise and multiple reflections from the wall of the pipe.

The system performs nondestructive monitoring through the walls of steam pipes, and automatically measures the height of condensed water while operating at the high-temperature conditions of 250 °C. For this purpose, the ultrasonic pulse-echo method is used where the time-of-flight of the wave reflections inside the water are measured, and it is multiplied by the wave velocity to determine the height. The pulse-echo test consists of emitting ultrasonic wave pulses from a piezoelectric transducer and receiving the reflections from the top and bottom of the condensed water. A single transducer is used as a transmitter as well as the receiver of the ultrasonic waves. To



The testbed simulating the Steam Pipe and the *in situ* ultrasonic test setup.

obtain high resolution, a broadband transducer is used and the frequency can be in the range of 2.25 to 10 MHz, providing sharp pulses in the time domain allowing for higher resolution in identifying the individual reflections.

The pulse-echo transducer is connected to both the transmitter (function generator), which sends electric signals to generate the elastic wave, and the receiver, which amplifies the attenuated reflected waves that are converted to electric signals. To avoid damage to the receiver, the large signal from the generator is blocked by an electronic switching mechanism from reaching the receiving circuitry. To assure the operation of the transducer at the required temperature range, the piezoelectric transmitter/receiver is selected with a Curie temperature that is much higher. In addition, the system can be improved by introducing a

heat sink between the transducer and the steam pipe, reducing the temperature requirements on the transducer.

This work was done by Yoseph Bar-Cohen, Shyh-Shiuh Lih, Mircea Badescu, Xiaoqi Bao, Stewart Sherrit, James S. Scott, Julian O. Blois, and Scott E. Widholm of Caltech for NASA's Jet Propulsion Laboratory. Further information is contained in a TSP (see page 1).

In accordance with Public Law 96-517, the contractor has elected to retain title to this invention. Inquiries concerning rights for its commercial use should be addressed to:

*Innovative Technology Assets Management
JPL*

*Mail Stop 202-233
4800 Oak Grove Drive
Pasadena, CA 91109-8099
E-mail: iaoffice@jpl.nasa.gov*

Refer to NPO-47518, volume and number of this NASA Tech Briefs issue, and the page number.

Control Program and Optical Improvements of Fresnel Microspectrometer

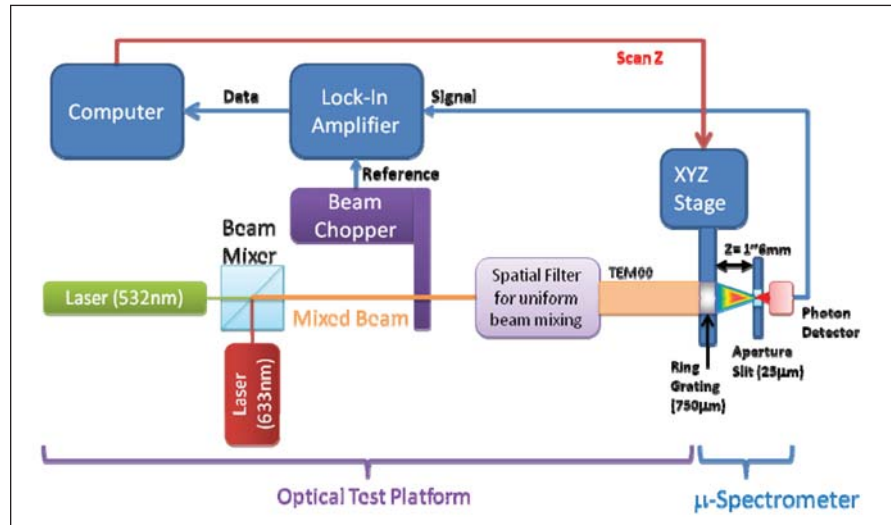
This innovation is suitable for optical fiber communications and medical applications where multiple optical fibers are used.

Langley Research Center, Hampton, Virginia

A microspectrometer has a circular geometry, and is designed with the Fresnel diffraction equation. This enables a dramatic miniaturization of the optical parts of a spectrometer over 100 times by volume. Therefore, it enables the construction of spectrometer arrays such as 100×100 microspectrometers for tunable multispectral or hyper-spectral imaging. It can be used for a massive, simultaneous spectral scan from multiple optical sources such as 10,000 optical fibers.

Two laser beams of 532 nm (green) and 633 nm (red) wavelengths were mixed and combined at a beam mixer. After the beam mixing, the beam looks like a yellow color to a human eye. This mixed pseudo-yellow beam passes a beam chopper operating at 191 Hz to modulate the beam for the lock-in amplification. A spatial filter was used to get a uniformly mixed TEM₀₀ beam in a wide beam diameter of about 1 cm. Then, the mixed beam enters the Fresnel ring grating whose diameter is only 750 μm. The ring grating separates the lights according to the wavelengths, and only the selected photons of the desired wavelength can pass the aperture slit of 25 μm in diameter.

The number of passed photons is measured as the current of a photon detector. The signal current is delivered to



The configuration of the optical test platform and the Microspectrometer.

the lock-in amplifier. The lock-in amplifier picks up only the 191 Hz frequency-locked signal from photon detector with respect to the reference signal from the beam chopper, and it rejects unwanted room lights and other stray lights. The computer receives the data from the lock-in amplifier and sends commands to an XYZ stage actuator to change the optical distance Z, between the ring grating and the aperture slit. A spectral scan is made with the linear actuator movement. The sharpness of the focal point

and the spectral resolving power were increased with the increasing numbers of rings in the grating.

Because the size of each microspectrometer is small, a dense array of spectrometers can be fabricated in a small area. Such an array can simultaneously capture the multiple spectral signals from various sources.

This work was done by Yeonjoon Park, Glen King, Sang Choi, and James Elliott of Langley Research Center. Further information is contained in a TSP (see page 1). LAR-17661-1

Miniature Laser Magnetometer

This device can be used for satellite, aircraft, and ground-based magnetic field sensors.

Goddard Space Flight Center, Greenbelt, Maryland

A conceptual design has been developed for a miniature laser magnetometer (MLM) that will measure the scalar magnitude and vector components of near-Earth magnetic fields. The MLM incorporates a number of technical innovations to achieve high-accuracy and high-resolution performance while significantly reducing the size of the laser-pumped helium magnetometer for use on small satellites and unmanned aerial vehicles (UAVs). The MLM will have a

dynamic range up to 75,000 nT. The scalar sensitivity will be 1 pT(Hz)^{-1/2} at 1 Hz with an accuracy of 0.2 nT. The vector sensitivity will be 1 pT(Hz)^{-1/2} at 1 Hz with an accuracy of 0.5 nT.

Fluxgates are the most common vector magnetometers used in space applications. They suffer from variable gain and offset drifts that significantly limit absolute accuracy for demanding scientific investigations of magnetic fields. MLM's helium magnetometer technol-

ogy is significantly more stable and accurate than these fluxgate magnetometers.

On satellites that include vector magnetometers, a separate reference scalar magnetometer is often included to correct the gains, offsets, and alignment errors of the vector instrument. The MLM will provide both scalar and self-calibrated vector measurements of the magnetic fields in a single instrument.

The MLM is a single magnetometer instrument consisting of separate sensor

and electronics sections that has the capability of measuring both the scalar magnetic field magnitude and the vector magnetic field components. Furthermore, the high-accuracy scalar measurements are used to calibrate and correct the vector component measurements in order to achieve superior vector accuracy and stability. The correction algorithm applied to the vector components for calibration and the same cell for vector and scalar measurements are major innovations. The separate sensor and electronics section of the MLM instrument allow the sensor to be installed on a boom or otherwise located away from electronics and other noisy magnetic components.

The MLM's miniaturization will be accomplished through the use of advanced

miniaturized components and packaging methods for the MLM sensor and electronics. The MLM conceptual design includes three key innovations. The first is a new non-magnetic laser package that will allow the placement of the laser pump source near the helium cell sensing elements. The second innovation is the design of compact, nested, triaxial Braubek coils used in the vector measurements that reduce the coil size by a factor of two compared to existing Helmholtz coils with similar field-generation performance. The third innovation is a compact sensor design that reduces the sensor volume by a factor of eight compared to MLM's predecessor.

The MLM design utilizes two distinct methods for performing scalar and vector measurements of magnetic fields.

For scalar measurements, the MLM uses the magnetically driven spin precession (MSP) technique where a coil near the helium cell sensing element is driven with a signal oscillating at the Larmor frequency. The signals from three orthogonal cells are summed to obtain omnidirectional sensitivity. For vector measurements, the MLM uses the bias field nulling (BFN) technique where orthogonal coil sets around one cell are used to null the magnetic field. The magnetic vector components are then proportional to the current required to null the field in the cell.

This work was done by Robert Slocum and Andy Brown of Polatomic Inc. for Goddard Space Flight Center. Further information is contained in a TSP (see page 1). GSC-16115-1



➤ Finding Every Root of a Broad Class of Real, Continuous Functions in a Given Interval

This robust and reliable algorithm is capable of locating the zeros of a continuous, nonlinear function.

NASA's Jet Propulsion Laboratory, Pasadena, California

One of the most pervasive needs within the Deep Space Network (DSN) Metric Prediction Generator (MPG) view period event generation is that of finding solutions to given occurrence conditions. While the general form of an equation expresses equivalence between its left-hand and right-hand expressions, the traditional treatment of the subject subtracts the two sides, leaving an expression of the form $f(x) = 0$. Values of the independent variable x satisfying this condition are roots, or solutions. Generally speaking, there may be no solutions, a unique solution, multiple solutions, or a continuum of solutions to a given equation.

In particular, all view period events are modeled as zero crossings of various metrics; for example, the time at which the elevation of a spacecraft reaches its maximum value, as viewed from a Deep Space Station (DSS), is found by locating that point at which the derivative of the eleva-

tion function becomes zero. Moreover, each event type may have several occurrences within a given time interval of interest. For example, a spacecraft in a low Moon orbit will experience several possible occultations per day, each of which must be located in time. The MPG is charged with finding all specified event occurrences that take place within a given time interval (or "pass"), without any special clues from operators as to when they may occur, for the entire spectrum of missions undertaken by the DSN. For each event type, the event metric function is a known form that can be computed for any instant within the interval.

A method has been created for a mathematical root finder to be capable of finding all roots of an arbitrary continuous function, within a given interval, to be subject to very lenient, parameterized assumptions. One assumption is that adjacent roots are separated at least by a given amount, $xGuard$. Any point

whose function value is less than ϵf in magnitude is considered to be a root, and the function values at distances $xGuard$ away from a root are larger than ϵf , unless there is another root located in this vicinity. A root is considered found if, during iteration, two root candidates differ by less than a pre-specified ϵx , and the optimum cubic polynomial matching the function at the end and at two interval points (that is within a relative error fraction ϵL at its midpoint) is reliable in indicating whether the function has extrema within the interval. The robustness of this method depends solely on choosing these four parameters that control the search. The roots of discontinuous functions were also found, but at degraded performance.

This work was done by Robert C. Tausworthe of SCT, Inc. and Paul A. Wolgast of Caltech for NASA's Jet Propulsion Laboratory. For more information, contact iaoffice@jpl.nasa.gov. NPO-46901

➤ Kalman Orbit Optimized Loop Tracking

This method has application in military GNSS receivers.

NASA's Jet Propulsion Laboratory, Pasadena, California

Under certain conditions of low signal power and/or high noise, there is insufficient signal to noise ratio (SNR) to close tracking loops with individual signals on orbiting Global Navigation Satellite System (GNSS) receivers. In addition, the processing power available from flight computers is not great enough to implement a conventional ultra-tight coupling tracking loop. This work provides a method to track GNSS signals at very low SNR without the penalty of requiring very high processor throughput to calculate the loop parameters.

The Kalman Orbit-Optimized Loop (KOOL) tracking approach constitutes a filter with a dynamic model and using the

aggregate of information from all tracked GNSS signals to close the tracking loop for each signal. For applications where there is not a good dynamic model, such as very low orbits where atmospheric drag models may not be adequate to achieve the required accuracy, aiding from an IMU (inertial measurement unit) or other sensor will be added. The KOOL approach is based on research JPL has done to allow signal recovery from weak and scintillating signals observed during the use of GPS signals for limb sounding of the Earth's atmosphere. That approach uses the onboard PVT (position, velocity, time) solution to generate predictions for the range, range rate, and ac-

celeration of the low-SNR signal. The low-SNR signal data are captured by a directed open loop. KOOL builds on the previous open loop tracking by including feedback and observable generation from the weak-signal channels so that the MSR receiver will continue to track and provide PVT, range, and Doppler data, even when all channels have low SNR.

The KOOL algorithm will also reduce the processor throughput requirements. This is enabled because the dynamic model of the receiver motion is very smooth, so that the full physical orbit model can be run at a low rate; for example, every 10 seconds. This contrasts with the signal tracking loop requirement for

a much less complex set of processor activity at 50 Hz, a 500 times higher rate. Coarse benchmarks of PVT filter requirements for processor throughput, and the benchmark tracking loop's requirements, indicate KOOL tracking will require an order of magnitude less

throughput, considering both its lower rate and greater complexity.

KOOL tracking high-rate models for phase and range at shorter times will be generated within the digital logic once they are primed with model parameters from the PVT filter. The onboard oscil-

lator must be commensurately stable, requiring $(\Delta F)/F$ of about 10^{-11} over times up to 10 seconds.

This work was done by Lawrence E. Young and Thomas K Meehan of Caltech for NASA's Jet Propulsion Laboratory. For more information, contact iaoffice@jpl.nasa.gov. NPO-46973

Development of Jet Noise Power Spectral Laws

This model can be used in measuring high-temperature steam pipes, leak noise from high-pressure pipes, or any device that generates noise by jet exhaust.

John H. Glenn Research Center, Cleveland, Ohio

High-quality jet noise spectral data measured at the Aero-Acoustic Propulsion Laboratory (AAPL) at NASA Glenn is used to develop jet noise scaling laws. A FORTRAN algorithm was written that provides detailed spectral prediction of component jet noise at user-specified conditions. The model generates quick estimates of the jet mixing noise and the broadband shock-associated noise (BBSN) in single-stream, axis-symmetric jets within a wide range of nozzle operating conditions.

Shock noise is emitted when supersonic jets exit a nozzle at imperfectly expanded conditions. A successful scaling of the BBSN allows for this noise component to be predicted in both convergent and convergent-divergent nozzles.

Configurations considered in this study consisted of convergent and convergent-divergent nozzles. Velocity exponents for the jet mixing noise were

evaluated as a function of observer angle and jet temperature. Similar intensity laws were developed for the broadband shock-associated noise in supersonic jets.

A computer program called "sJet" was developed that provides a quick estimate of component noise in single-stream jets at a wide range of operating conditions. A number of features have been incorporated into the data bank and subsequent scaling in order to improve jet noise predictions. Measurements have been converted to a lossless format. Set points have been carefully selected to minimize the instability-related noise at small aft angles. Regression parameters have been scrutinized for error bounds at each angle. Screech-related amplification noise has been kept to a minimum to ensure that the velocity exponents for the jet mixing noise remain free of amplifications. A shock-noise-intensity scal-

ing has been developed independent of the nozzle design point.

The computer program provides detailed narrow-band spectral predictions for component noise (mixing noise and shock associated noise), as well as the total noise. Although the methodology is confined to single streams, efforts are underway to generate a data bank and algorithm applicable to dual-stream jets. Shock-associated noise in high-powered jets such as military aircraft can benefit from these predictions.

This work was done by Abbas Khavaran and James Bridges of Glenn Research Center. Further information is contained in a TSP (see page 1).

Inquiries concerning rights for the commercial use of this invention should be addressed to NASA Glenn Research Center, Innovative Partnerships Office, Attn: Steven Fedor, Mail Stop 4-8, 21000 Brookpark Road, Cleveland, Ohio 44135. Refer to LEW-18600-1.



GLobal Integrated Design Environment

John H. Glenn Research Center, Cleveland, Ohio

The GLobal Integrated Design Environment (GLIDE) is a collaborative engineering application built to resolve the design session issues of real-time passing of data between multiple discipline experts in a collaborative environment. Utilizing Web protocols and multiple programming languages, GLIDE allows engineers to use the applications to which they are accustomed — in this case, Excel — to send and receive datasets via the Internet to a database-driven Web server.

Traditionally, a collaborative design session consists of one or more engineers representing each discipline meeting together in a single location. The discipline leads exchange parameters and iterate through their respective processes to converge on an acceptable

dataset. In cases in which the engineers are unable to meet, their parameters are passed via e-mail, telephone, facsimile, or even postal mail. The result of this slow process of data exchange would elongate a design session to weeks or even months. While the iterative process remains in place, software can now exchange parameters securely and efficiently, while at the same time allowing for much more information about a design session to be made available.

GLIDE is written in a compilation of several programming languages, including REALbasic, PHP, and Microsoft Visual Basic. GLIDE client installers are available to download for both Microsoft Windows and Macintosh systems. The GLIDE client software is compatible with Microsoft Excel 2000

or later on Windows systems, and with Microsoft Excel X or later on Macintosh systems.

GLIDE follows the Client-Server paradigm, transferring encrypted and compressed data via standard Web protocols. Currently, the engineers use Excel as a front end to the GLIDE Client, as many of their custom tools run in Excel.

This work was done by Matthew Kunkel, Melissa McGuire, David A. Smith, and Leon P. Gefert of Glenn Research Center. Further information is contained in a TSP (see page 1).

Inquiries concerning rights for the commercial use of this invention should be addressed to NASA Glenn Research Center, Innovative Partnerships Office, Attn: Steven Fedor, Mail Stop 4-8, 21000 Brookpark Road, Cleveland, Ohio 44135. Refer to LEW-18591-1.

SSC Engineering Analysis

Stennis Space Center, Mississippi

A package for the automation of the Engineering Analysis (EA) process at the Stennis Space Center has been customized. It provides the ability to assign and track analysis tasks electronically, and electronically route a task for approval. It now provides a mechanism to keep these analyses under configuration management. It also allows the analysis to be stored and linked to the engineering data that is needed to perform the analysis (drawings, etc.). PTC's (Parametric Technology Corporation) Windchill product was customized to allow the EA to be created, routed, and maintained under con-

figuration management. Using Info-engine Tasks, JSP (JavaServer Pages), Javascript, a user interface was created within the Windchill product that allows users to create EAs. Not only does this interface allow users to create and track EAs, but it plugs directly into the out-of-the-box ability to associate these analyses with other relevant engineering data such as drawings. Also, using the Windchill workflow tool, the Design and Data Management System (DDMS) team created an electronic routing process based on the manual/informal approval process. The team also added the ability

for users to notify and track notifications to individuals about the EA.

Prior to the Engineering Analysis creation, there was no electronic way of creating and tracking these analyses. There was also a feature that was added that would allow users to track/log e-mail notifications of the EA.

This work was done by Harry Ryan and Justin Junell of Stennis Space Center; Colby Albasini of Computer Sciences Corporation; and William O'Rourke, Thang Le, Ted Strain, and Tim Stiglets of SaiTech. For more information call the SSC Center Chief Technologist at (228) 688-1929. Refer to SSC-00340.

Automated Cryocooler Monitor and Control System Software

NASA's Jet Propulsion Laboratory, Pasadena, California

This software is used in an automated cryogenic control system developed to monitor and control the operation of small-scale cryocoolers. The system was designed to automate the cryogenically

cooled low-noise amplifier system described in "Automated Cryocooler Monitor and Control System" (NPO-47246), *NASA Tech Briefs*, Vol. 35, No. 5 (May 2011), page 7a.

The software contains algorithms necessary to convert non-linear output voltages from the cryogenic diode-type thermometers and vacuum pressure and helium pressure sensors, to temperature

and pressure units. The control function algorithms use the monitor data to control the cooler power, vacuum solenoid, vacuum pump, and electrical warm-up heaters. The control algorithms are based on a rule-based system that activates the required device based on the

operating mode. The external interface is Web-based. It acts as a Web server, providing pages for monitor, control, and configuration. No client software from the external user is required.

This work was done by Michael J. Britcliffe, Bruce L. Conroy, Paul E. Anderson, and

Ahmad Wilson of Caltech for NASA's Jet Propulsion Laboratory. Further information is contained in a TSP (see page 1).

This software is available for commercial licensing. Please contact Daniel Broderick of the California Institute of Technology at danielb@caltech.edu. Refer to NPO-47247.

Common Bolted Joint Analysis Tool

Lyndon B. Johnson Space Center, Houston, Texas

Common Bolted Joint Analysis Tool (comBAT) is an Excel/VB-based bolted joint analysis/optimization program that lays out a systematic foundation for an inexperienced or seasoned analyst to determine fastener size, material, and assembly torque for a given design. Analysts are able to perform numerous "what-if" scenarios within minutes to arrive at an optimal solution. The program evaluates input design parameters, performs joint assembly checks, and steps through numerous calculations to arrive at several key margins of safety for each member in a joint. It also checks for joint gapping,

provides fatigue calculations, and generates joint diagrams for a visual reference. Optimum fastener size and material, as well as correct torque, can then be provided.

Analysis methodology, equations, and guidelines are provided throughout the solution sequence so that this program does not become a "black box" for the analyst. There are built-in databases that reduce the legwork required by the analyst. Each step is clearly identified and results are provided in number format, as well as color-coded spelled-out words to draw user attention.

The three key features of the software are robust technical content, innovative and user friendly I/O, and a large database. The program addresses every aspect of bolted joint analysis and proves to be an instructional tool at the same time. It saves analysis time, has intelligent messaging features, and catches operator errors in real time.

This work was done by Kauser Imtiaz of The Boeing Co. for Johnson Space Center. For further information, contact the JSC Innovative Partnerships Office at (281) 483-3809. MSC-24836-1

Draper Station Analysis Tool

Lyndon B. Johnson Space Center, Houston, Texas

Draper Station Analysis Tool (DSAT) is a computer program, built on commercially available software, for simulating and analyzing complex dynamic systems. Heretofore used in designing and verifying guidance, navigation, and control systems of the International Space Station, DSAT has a modular architecture that lends itself to modification for application to spacecraft or terrestrial systems. DSAT consists of user-interface, data-structures, simulation-generation, analysis, plotting, documentation, and help components. DSAT automates the construction of sim-

ulations and the process of analysis. DSAT provides a graphical user interface (GUI), plus a Web-enabled interface, similar to the GUI, that enables a remotely located user to gain access to the full capabilities of DSAT via the Internet and Web-browser software. Data structures are used to define the GUI, the Web-enabled interface, simulations, and analyses. Three data structures define the type of analysis to be performed: closed-loop simulation, frequency response, and/or stability margins. DSAT can be executed on almost any workstation, desktop, or laptop com-

puter. DSAT provides better than an order of magnitude improvement in cost, schedule, and risk assessment for simulation based design and verification of complex dynamic systems.

This program was written by Nazareth Bedrossian, Jiann-Woei Jang, Edward McCants, Zachary Omohundro, Tom Ring, Jeremy Templeton, Jeremy Zoss, Jonathan Wallace, and Philip Ziegler of Charles Stark Draper Laboratory, Inc., for Johnson Space Center. For further information, contact the Johnson Commercial Technology Office at (281) 483-3809. MSC-23607-1

Commercial Modular Aero-Propulsion System Simulation 40k

John H. Glenn Research Center, Cleveland, Ohio

The Commercial Modular Aero-Propulsion System Simulation 40k (C-MAPSS40k) software package is a non-linear dynamic simulation of a 40,000-pound (≈ 178 -kN) thrust class commercial turbofan engine, written in the MATLAB/Simulink environment.

The model has been tuned to capture the behavior of flight test data, and is capable of running at any point in the flight envelope [up to 40,000 ft ($\approx 12,200$ m) and Mach 0.8]. In addition to the open-loop engine, the simulation includes a controller whose ar-

chitecture is representative of that found in industry.

The simulation environment gives the user easy access to health, control, and engine parameters. C-MAPSS40k has a graphical user interface (GUI) to allow users to easily specify an arbitrarily com-

plex flight profile to be simulated, as well as ambient conditions and deterioration level of the engine. C-MAPSS40k has three actuators: fuel flow, variable stator vanes, and variable bleed valve. The three actuators enable off-nominal operation, which is not possible with simulations that have fuel flow as the sole actuator, since in those simulations the other actuators are implicit and assumed to operate nominally. The simulation is modular to allow users to re-design or replace components such as the engine controller or turbomachinery components without having to modify the rest of the simulation. It also enables the user to view and save any signal

in the engine or controller. The package has the capability to create and validate a linear model of the engine at any operating point. Linear models can be used for control design, and C-MAPSS40k lends itself well to implementation and evaluation of advanced control designs as well as to diagnostic and prognostic system development. The simulation can be run in real time and can therefore be integrated into a flight simulator with a pilot in the loop for testing.

C-MAPSS40k fills the need for an easy-to-use, realistic, transient simulation of a medium-size commercial turbofan engine with a representative controller. It is a detailed component level model

(CLM) written in the industry-standard graphical MATLAB/Simulink environment to allow for easy modification and portability. At the time of this reporting, no other such model exists in the public domain.

This work was done by Ten-Huei Guo, Thomas Lavelle, and Jonathan Litt of Glenn Research Center and Jeffrey Csank of N&R Engineering and Ryan May of ASRC. Further information is contained in a TSP (see page 1).

Inquiries concerning rights for the commercial use of this invention should be addressed to NASA Glenn Research Center, Innovative Partnerships Office, Attn: Steven Fedor, Mail Stop 4-8, 21000 Brookpark Road, Cleveland, Ohio 44135. Refer to LEW-18624-1.

The Planning Execution Monitoring Architecture

Lyndon B. Johnson Space Center, Houston, Texas

The Planning Execution Monitoring (PEM) architecture is a design concept for developing autonomous cockpit command and control software. The PEM architecture is designed to reduce the operations costs in the space transportation system through the use of automation while improving safety and operability of the system. Specifically, the PEM autonomous framework enables automatic performance of many vehicle operations that would typically be performed by a human. Also, this framework supports varying levels of autonomous control, ranging from fully automatic to fully manual control.

The PEM autonomous framework interfaces with the “core” flight software to perform flight procedures. It can either

assist human operators in performing procedures or autonomously execute routine cockpit procedures based on the operational context. Most importantly, the PEM autonomous framework promotes and simplifies the capture, verification, and validation of the flight operations knowledge. Through a hierarchical decomposition of the domain knowledge, the vehicle command and control capabilities are divided into manageable functional “chunks” that can be captured and verified separately. These functional units, each of which has the responsibility to manage part of the vehicle command and control, are modular, re-usable, and extensible. Also, the functional units are self-contained and have the ability to plan and

execute the necessary steps for accomplishing a task based upon the current mission state and available resources.

The PEM architecture has potential for application outside the realm of spaceflight, including management of complex industrial processes, nuclear control, and control of complex vehicles such as submarines or unmanned air vehicles.

This work was done by Lui Wang, Bebe Ly, and Alan Crocker of Johnson Space Center; Debra Schreckenghost of Metrica Inc; Stephen Mueller and Bob Phillips of Titan-LinCom Corp.; and David Wadsworth and Charles Sorensen of Lockheed Martin Corp. For further information, contact the Johnson Commercial Technology Office at (281) 483-3809. MSC-23628-1

Jitter Controller Software

Lyndon B. Johnson Space Center, Houston, Texas

Sinusoidal jitter is produced by simply modulating a clock frequency sinusoidally with a given frequency and amplitude. But this can be expressed as phase jitter, frequency jitter, or cycle-to-cycle jitter, rms or peak, absolute units, or normalized to the base clock frequency. Jitter using other waveforms requires calculating and downloading these waveforms to an arbitrary waveform generator, and helping the user manage relationships among phase jitter crest factor, frequency jitter crest factor, and cycle-to-cycle jitter (CCJ) crest factor.

Software was developed for managing these relationships, automatically configuring the generator, and saving test results documentation. Tighter management of clock jitter and jitter sensitivity is required by new codes that further extend the already high performance of space communication links, completely correcting symbol error rates higher than 10 percent, and therefore typically requiring demodulation and symbol synchronization hardware to operating at signal-to-noise ratios of less than one. To accomplish this,

greater demands are also made on transmitter performance, and measurement techniques are needed to confirm performance. It was discovered early that sinusoidal jitter can be stepped on a grid such that one can connect points by constant phase jitter, constant frequency jitter, or constant cycle-cycle jitter. The tool automates adherence to a grid while also allowing adjustments off-grid. Also, the jitter can be set by the user on any dimension and the others are calculated. The calculations are all recorded, allowing the data to be rap-

idly plotted or re-plotted against different interpretations just by changing pointers to columns.

A key advantage is taking data on a carefully controlled grid, which allowed a single data set to be post-analyzed many different ways. Another innovation was building a software tool to provide very tight coupling between the generator and the recorded data prod-

uct, and the operator's worksheet. Together, these allowed the operator to sweep the jitter stimulus quickly along any of three dimensions and focus on the response of the system under test (response was jitter transfer ratio, or performance degradation to the symbol or codeword error rate). Additionally, managing multi-tone and noise waveforms automated a tedious manual process,

and provided almost instantaneous decision-making control over test flow. The code was written in LabVIEW, and calls Agilent instrument drivers to write to the generator hardware.

This work was done by Chatwin Lansdowne and Adam Schlesinger of Johnson Space Center. Further information is contained in a TSP (see page 1). MSC-24814-1



μShell Minimalist Shell for Xilinx Microprocessors

NASA's Jet Propulsion Laboratory, Pasadena, California

μShell is a lightweight shell environment for engineers and software developers working with embedded microprocessors in Xilinx FPGAs. (μShell has also been successfully ported to run on ARM Cortex-M1 microprocessors in Actel ProASIC3 FPGAs, but without project-integration support.) μShell decreases the time spent performing initial tests of field-programmable gate array (FPGA) designs, simplifies running customizable one-time-only experiments, and provides a familiar-feeling command-line interface. The program comes with a collection of useful functions and enables the designer to add an unlimited number of custom commands, which are callable from the command-line. The commands are parameterizable (using the C-based command-line parameter idiom), so the designer can use one function to exercise hardware with different values. Also,

since many hardware peripherals instantiated in FPGAs have reasonably simple register-mapped I/O interfaces, the engineer can edit and view hardware parameter settings at any time without stopping the processor.

μShell comes with a set of support scripts that interface seamlessly with Xilinx's EDK tool. Adding an instance of μShell to a project is as simple as marking a check box in a library configuration dialog box and specifying a software project directory. The support scripts then examine the hardware design, build design-specific functions, conditionally include processor-specific functions, and complete the compilation process. For code-size constrained designs, most of the stock functionality can be excluded from the compiled library.

When all of the configurable options are removed from the binary, μShell has an unoptimized memory footprint of

about 4.8 kB and a size-optimized footprint of about 2.3 kB. Since μShell allows unfettered access to all processor-accessible memory locations, it is possible to perform live patching on a running system. This can be useful, for instance, if a bug is discovered in a routine but the system cannot be rebooted: μShell allows a skilled operator to directly edit the binary executable in memory. With some forethought, μShell code can be located in a different memory location from custom code, permitting the custom functionality to be overwritten at any time without stopping the controlling shell.

This work was done by Thomas A. Werne of Caltech for NASA's Jet Propulsion Laboratory. Further information is contained in a TSP (see page 1).

This software is available for commercial licensing. Please contact Daniel Broderick of the California Institute of Technology at danielb@caltech.edu. Refer to NPO-47495.



Software Displays Data on Active Regions of the Sun

Lyndon B. Johnson Space Center, Houston, Texas

The Solar Active Region Display System is a computer program that generates, in near real time, a graphical display of parameters indicative of the spatial and temporal variations of activity on the Sun. These parameters include histories and distributions of solar flares, active region growth, coronal mass ejections, size, and magnetic configuration.

By presenting solar-activity data in graphical form, this program accelerates, facilitates, and partly automates what had previously been a time-consuming mental process of interpretation of solar-activity data presented in tabular and textual formats. Intended for origi-

nal use in predicting space weather in order to minimize the exposure of astronauts to ionizing radiation, the program might also be useful on Earth for predicting solar-wind-induced ionospheric effects, electric currents, and potentials that could affect radio-communication systems, navigation systems, pipelines, and long electric-power lines.

Raw data for the display are obtained automatically from the Space Environment Center (SEC) of the National Oceanic and Atmospheric Administration (NOAA). Other data must be obtained from the NOAA SEC by verbal communication and entered manually. The Solar Active Region Display System

automatically accounts for the latitude dependence of the rate of rotation of the Sun, by use of a mathematical model that is corrected with NOAA SEC active-region position data once every 24 hours. The display includes the date, time, and an image of the Sun in H α light overlaid with latitude and longitude coordinate lines, dots that mark locations of active regions identified by NOAA, identifying numbers assigned by NOAA to such regions, and solar-region visual summary (SRVS) indicators associated with some of the active regions.

Each SRVS indicator is a small pie chart containing five equal sectors, each

of which is color-coded to provide a semiquantitative indication of the degree of hazard posed by one aspect of the activity at the indicated location. The five aspects in question are the history of solar flares, the history of coronal mass ejections, the growth or decay of activity, the overall size, and the magnetic configuration.

Mouse-clicking on an active-region-marking dot, SRVS indicator, or NOAA

region number causes the program to generate a solar-region summary table (SRT) for the active region in question. The SRT contains additional quantitative and qualitative data, beyond those contained in the SRVS: These data include the solar coordinates of the region, the area of the region and its change in area during the past 24 hours, the change in the number of sunspots in the region during the past

24 hours, the magnetic configuration, and the types, dates, and times of the most recent flare and coronal mass ejection.

This program was written by Mike Golithly of Johnson Space Center, Mark Weyland of Lockheed Martin, and Vern Raben of Raben Systems, Inc. For further information, contact the JSC Innovation Partnerships Office at (281) 483-3809. MSC-23300-1

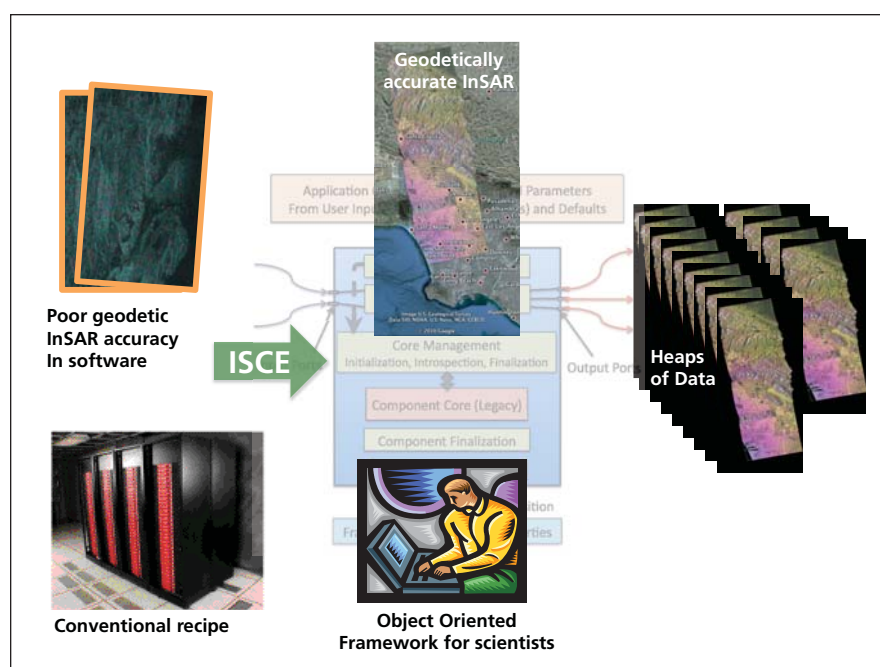
InSAR Scientific Computing Environment

NASA's Jet Propulsion Laboratory, Pasadena, California

This computing environment is the next generation of geodetic image processing technology for repeat-pass Interferometric Synthetic Aperture (InSAR) sensors, identified by the community as a needed capability to provide flexibility and extensibility in reducing measurements from radar satellites and aircraft to new geophysical products. This software allows users of interferometric radar data the flexibility to process from Level 0 to Level 4 products using a variety of algorithms and for a range of available sensors.

There are many radar satellites in orbit today delivering to the science community data of unprecedented quantity and quality, making possible large-scale studies in climate research, natural hazards, and the Earth's ecosystem. The proposed DESDynI mission, now under consideration by NASA for launch later in this decade, would provide time series and multi-image measurements that permit 4D models of Earth surface processes so that, for example, climate-induced changes over time would become apparent and quantifiable. This advanced data processing technology, applied to a global data set such as from the proposed DESDynI mission, enables a new class of analyses at time and spatial scales unavailable using current approaches.

This software implements an accurate, extensible, and modular processing system designed to realize the full potential of InSAR data from future missions such as the proposed DESDynI, existing radar satellite data, as well as data from the NASA UAVSAR (Uninhabited Aerial Vehicle Synthetic Aperture Radar), and other airborne platforms. The processing approach



The **InSAR Scientific Computing Environment (ISCE)** replaces old InSAR processing algorithms and conventional computing paradigms with modern geodetically accurate algorithms embedded at the core of a modern, flexible, and extensible object-oriented computing framework. The framework enables scientists to easily and efficiently process raw data into useful data products for their science models and investigations.

has been re-thought in order to enable multi-scene analysis by adding new algorithms and data interfaces, to permit user-reconfigurable operation and extensibility, and to capitalize on codes already developed by NASA and the science community. The framework incorporates modern programming methods based on recent research, including object-oriented scripts controlling legacy and new codes, abstraction and generalization of the data model for efficient manipulation of objects among modules, and well-designed module interfaces suitable for command-line execution or GUI-program-

ming. The framework is designed to allow users' contributions to promote maximum utility and sophistication of the code, creating an open-source community that could extend the framework into the indefinite future.

This work was done by Paul A. Rosen, Gian Franco Sacco, and Eric M. Gurrola of JPL/Caltech; and Howard A. Zebker of Stanford University for NASA's Jet Propulsion Laboratory. Further information is contained in a TSP (see page 1).

This software is available for commercial licensing. Please contact Daniel Broderick of the California Institute of Technology at danielb@caltech.edu. Refer to NPO-47557.

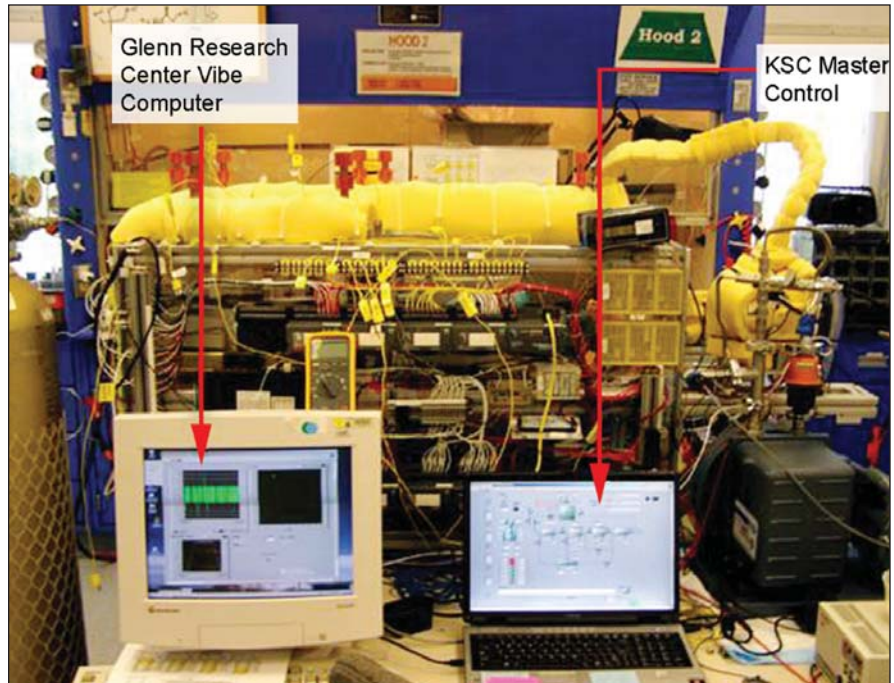
Software Architecture to Support the Evolution of the ISRU RESOLVE Engineering Breadboard Unit 2 (EBU2)

John F. Kennedy Space Center, Florida

The In-Situ Resource Utilization (ISRU) Regolith & Environmental Science and Oxygen & Lunar Volatiles Extraction (RESOLVE) software provides operation of the physical plant from a remote location with a high-level interface that can access and control the data from external software applications of other subsystems. This software allows autonomous control over the entire system with manual computer control of individual system/process components. It gives non-programmer operators the capability to easily modify the high-level autonomous sequencing while the software is in operation, as well as the ability to modify the low-level, file-based sequences prior to the system operation. Local automated control in a distributed system is also enabled where component control is maintained during the loss of network connectivity with the remote workstation. This innovation also minimizes network traffic.

The software architecture commands and controls the latest generation of RESOLVE processes used to obtain, process, and quantify lunar regolith. The system is grouped into six sub-processes: Drill, Crush, Reactor, Lunar Water Resource Demonstration (LWRD), Regolith Volatiles Characterization (RVC) (see example), and Regolith Oxygen Extraction (ROE). Some processes are independent, some are dependent on other processes, and some are independent but run concurrently with other processes.

The first goal is to analyze the volatiles emanating from lunar regolith, such as water, carbon monoxide, carbon diox-



Integrated LWRD/RVC engineering breadboard unit showing computer controls.

ide, ammonia, hydrogen, and others. This is done by heating the soil and analyzing and capturing the volatilized product. The second goal is to produce water by reducing the soil at high temperatures with hydrogen. This is done by raising the reactor temperature in the range of 800 to 900 °C, causing the reaction to progress by adding hydrogen, and then capturing the water product in a desiccant bed.

The software needs to run the entire unit and all sub-processes; however, throughout testing, many variables and

parameters need to be changed as more is learned about the system operation. The Master Events Controller (MEC) is run on a standard laptop PC using Windows XP. This PC runs in parallel to another laptop that monitors the GC, and a third PC that monitors the drilling/crushing operation. These three PCs interface to the process through a CompactRIO, OPC Servers, and modems.

This work was done by Thomas Moss, Mark Nurge, and Stephen Perusich of Kennedy Space Center. Further information is contained in a TSP (see page 1). KSC-13353

Coastal On-line Assessment and Synthesis Tool 2.0

Stennis Space Center, Mississippi

COAST (Coastal On-line Assessment and Synthesis Tool) is a 3D, open-source Earth data browser developed by leveraging and enhancing previous NASA open-source tools. These tools use satellite imagery and elevation data in a way that allows any user to zoom from orbit view down into any place on Earth, and enables the user to experience Earth terrain in a visually rich 3D view. The bene-

fits associated with taking advantage of an open-source geo-browser are that it is free, extensible, and offers a worldwide developer community that is available to provide additional development and improvement potential.

What makes COAST unique is that it simplifies the process of locating and accessing data sources, and allows a user to combine them into a multi-layered

and/or multi-temporal visual analytical look into possible data interrelationships and coefficients for coastal environment phenomenology. COAST provides users with new data visual analytic capabilities. COAST has been upgraded to maximize use of open-source data access, viewing, and data manipulation software tools.

The COAST 2.0 toolset has been developed to increase access to a larger realm

of the most commonly implemented data formats used by the coastal science community. New and enhanced functionalities that upgrade COAST to COAST 2.0 include the development of the Temporal Visualization Tool (TVT) plug-in, the Recursive Online Remote Data-Data Mapper (RECORD-DM) utility, the Im-

port Data Tool (IDT), and the Add Points Tool (APT). With these improvements, users can integrate their own data with other data sources, and visualize the resulting layers of different data types (such as spatial and spectral, for simultaneous visual analysis), and visualize temporal changes in areas of interest.

This work was done by Richard Brown of Science Systems and Applications, Inc., Andrew Navard of Computer Sciences Corporation, and Beth Nguyen of Delta Computer Solutions for Stennis Space Center. For more information, contact the Office of Chief Technologist at Stennis Space Center, 228-688-1929. Refer to SSC-00357.

Generalized Software Architecture Applied to the Continuous Lunar Water Separation Process and the Lunar Greenhouse Amplifier

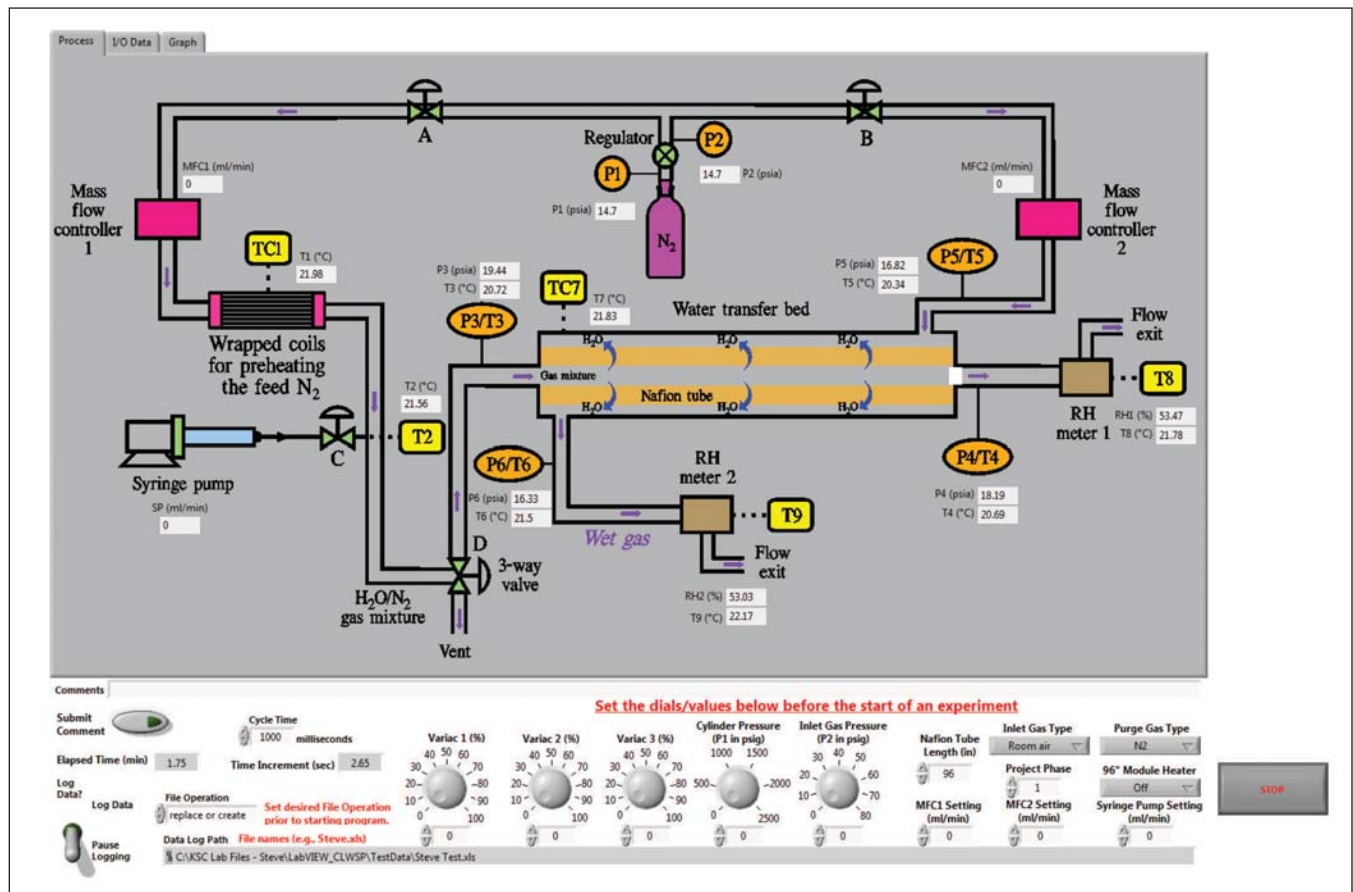
John F. Kennedy Space Center, Florida

This innovation provides the user with autonomous on-screen monitoring, embedded computations, and tabulated output for two new processes. The software was originally written for the Continuous Lunar Water Separation Process (CLWSP), but was found to be general enough to be applicable to the Lunar Greenhouse Amplifier (LGA) as well, with minor alterations. The resultant program should have general applicability to many laboratory processes (see figure).

The objective for these programs was to create a software application that would provide both autonomous monitoring and data storage, along with manual manipulation. The software also allows operators the ability to input experimental changes and comments in real time without modifying the code itself. Common process elements, such as thermocouples, pressure transducers, and relative humidity sensors, are easily incorporated into

the program in various configurations, along with specialized devices such as photodiode sensors.

The goal of the CLWSP research project is to design, build, and test a new method to continuously separate, capture, and quantify water from a gas stream. The application is any In-Situ Resource Utilization (ISRU) process that desires to extract or produce water from lunar or planetary regolith. The present work is aimed at circumventing



Sample Process

current problems and ultimately producing a system capable of continuous operation at moderate temperatures that can be scaled over a large capacity range depending on the ISRU process.

The goal of the LGA research project is to design, build, and test a new type of greenhouse that could be used on the moon or Mars. The LGA uses super greenhouse gases (SGGs) to absorb long-wavelength radiation, thus creating a highly efficient greenhouse at a future lunar or Mars outpost. Silica-based glass, although highly efficient at trapping heat, is heavy, fragile, and not suitable for space greenhouse applications.

Plastics are much lighter and resilient, but are not efficient for absorbing long-wavelength infrared radiation and therefore will lose more heat to the environment compared to glass. The LGA unit uses a transparent polymer “antechamber” that surrounds part of the greenhouse and encases the SGGs, thereby minimizing infrared losses through the plastic windows. With ambient temperatures at the lunar poles at $-50\text{ }^{\circ}\text{C}$, the LGA should provide a substantial enhancement to currently conceived lunar greenhouses. Positive results obtained from this project could lead to a future large-scale system capa-

ble of running autonomously on the Moon, Mars, and beyond.

The software for both applications needs to run the entire units and all sub-processes; however, throughout testing, many variables and parameters need to be changed as more is learned about the system operation. The software provides the versatility to permit the software operation to change as the user requirements evolve.

This work was done by Stephen Perusich, Thomas Moss, and Anthony Muscatello of Kennedy Space Center. Further information is contained in a TSP (see page 1). KSC-13539

Graphical Language for Data Processing

Stennis Space Center, Mississippi

A graphical language for processing data allows processing elements to be connected with virtual “wires” that represent data flows between processing modules. The processing of complex data, such as lidar data, requires many different algorithms to be applied. The purpose of this innovation is to automate the processing of complex data, such as LIDAR, without the need for complex scripting and programming languages.

The system consists of a set of user-interface components that allow the user to drag and drop various algorithmic and processing components onto a

process graph. By working graphically, the user can completely visualize the process flow and create complex diagrams. This innovation supports the nesting of graphs, such that a graph can be included in another graph as a single step for processing.

In addition to the user interface components, the system includes a set of .NET classes that represent the graph internally. These classes provide the internal system representation of the graphical user interface. The system includes a graph execution component that reads the internal representation of the graph (as described above) and

executes that graph. The execution of the graph follows the interpreted model of execution in that each node is traversed and executed from the original internal representation. In addition, there are components that allow external code elements, such as algorithms, to be easily integrated into the system, thus making the system infinitely expandable.

This work was done by Keith Alphonso of Diamond Data Systems for Stennis Space Center. For more information, contact Keith Alphonso, Director Diamond Data Systems, a Geocent Company at kalphonso@Geocent.com, (228) 688-3145. SSC-00324

Monitoring Areal Snow Cover Using NASA Satellite Imagery

Goddard Space Flight Center, Greenbelt, Maryland

The objective of this project is to develop products and tools to assist in the hydrologic modeling process, including tools to help prepare inputs for hydrologic models and improved methods for the visualization of streamflow forecasts. In addition, this project will facilitate the use of NASA satellite imagery (primarily snow cover imagery) by other federal and state agencies with operational streamflow forecasting responsibilities.

A GIS software toolkit for monitoring areal snow cover extent and producing streamflow forecasts is being developed. This toolkit will be packaged as multiple extensions for ArcGIS 9.x and an open-source GIS software package. The toolkit will provide users with a means

for ingesting NASA EOS satellite imagery (snow cover analysis), preparing hydrologic model inputs, and visualizing streamflow forecasts. Primary products include a software tool for predicting the presence of snow under clouds in satellite images; a software tool for producing gridded temperature and precipitation forecasts; and a suite of tools for visualizing hydrologic model forecasting results. The toolkit will be an expert system designed for operational users that need to generate accurate streamflow forecasts in a timely manner.

The Remote Sensing of Snow Cover Toolbar will ingest snow cover imagery from multiple sources, including the MODIS Operational Snowcover Data

and convert them to gridded datasets that can be readily used. Statistical techniques will then be applied to the gridded snow cover data to predict the presence of snow under cloud cover. The toolbar has the ability to ingest both binary and fractional snow cover data. Binary mapping techniques use a set of thresholds to determine whether a pixel contains snow or no snow. Fractional mapping techniques provide information regarding the percentage of each pixel that is covered with snow. After the imagery has been ingested, physiographic data is attached to each cell in the snow cover image. This data can be obtained from a digital elevation model (DEM) for the area of interest. If

the snow cover image contains cloud cover, regression tree analysis is used to predict the presence of snow cover under clouds.

The Gridded Temperature and Precipitation Forecast Toolbar will ingest forecasts from numerical weather prediction models and produce gridded forecasts that can be used as input for distributed hydrologic models. This toolbar will enable users to easily produce gridded fields of temperature and precipitation from location-specific forecasts, which is needed since a majority of hydrologic models are run on a distrib-

uted basis. This is completed using temperature data, and will be expanded in the future to include precipitation data.

The Streamflow Forecast Visualization Toolbar will generate visualizations of streamflow forecasts. Outputs include a variety of tables, charts, and figures depicting streamflow forecasts in formats that can be easily interpreted by the general public.

The interpolation process entails: (1) obtaining a DEM for the watershed (basin) of interest; (2) obtaining temperature (forecasted or observed) and elevation values for an individual

weather station (base station) located within the watershed; and (3) applying the monthly temperature lapse rates to create gridded values. After a DEM is selected for the area of interest, the GIS tools essentially complete the interpolation process for any specified day automatically. Tools are included to assist in the validation of the forecast grids.

This work was done by Brian J. Harshburger, Troy Blandford, and Brandon Moore of Aniak Consulting, LLC, for Goddard Space Flight Center. Further information is contained in a TSP (see page 1). GSC-15791-1

Adaptation of G-TAG Software for Validating Touch-and-Go Comet Surface Sampling Design Methodology

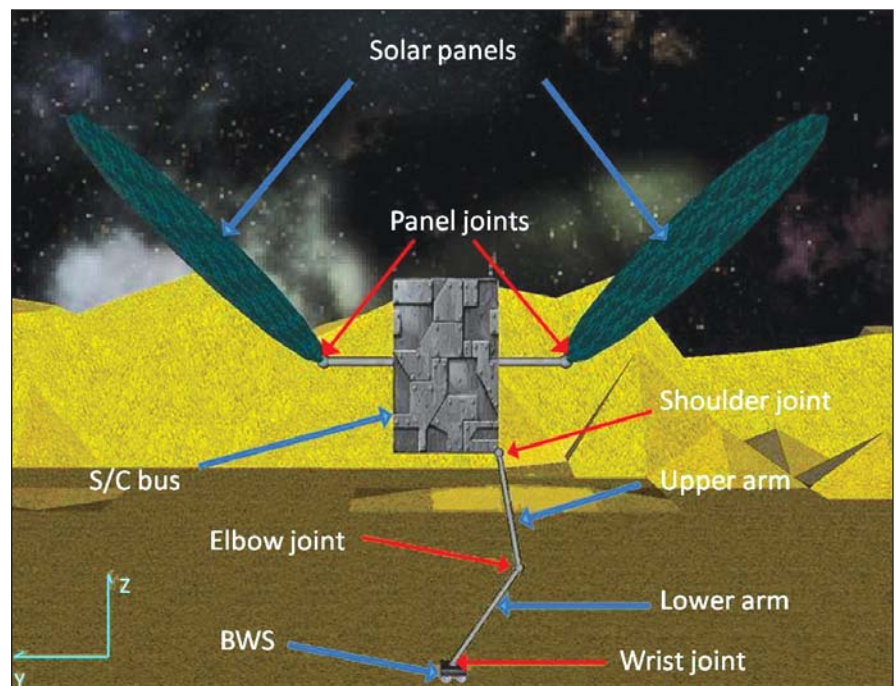
NASA's Jet Propulsion Laboratory, Pasadena, California

The G-TAG software tool was developed under the R&TD on Integrated Autonomous Guidance, Navigation, and Control for Comet Sample Return, and represents a novel, multi-body dynamics simulation software tool for studying TAG sampling.

The G-TAG multi-body simulation tool provides a simulation environment in which a Touch-and-Go (TAG) sampling event can be extensively tested. TAG sampling requires the spacecraft to descend to the surface, contact the surface with a sampling collection device, and then to ascend to a safe altitude. The TAG event lasts only a few seconds but is mission-critical with potentially high risk. Consequently, there is a need for the TAG event to be well characterized and studied by simulation and analysis in order for the proposal teams to converge on a reliable spacecraft design.

This adaptation of the G-TAG tool was developed to support the Comet Odyssey proposal effort, and is specifically focused to address comet sample return missions. In this application, the spacecraft descends to and samples from the surface of a comet. Performance of the spacecraft during TAG is assessed based on survivability and sample collection performance.

For the adaptation of the G-TAG simulation tool to comet scenarios, models are developed that accurately describe the properties of the spacecraft, approach trajectories, and descent velocities, as well as the models of the external forces and torques acting on the spacecraft. The adapted models of the space-



Comet Spacecraft Concept: Red arrows point to joints, blue arrows to spacecraft body components. The frame used for the simulation and for creating simulation movies is shown in the lower-left corner (x-axis completes coordinate system using the right-hand rule).

craft, descent profiles, and external sampling forces/torques were more sophisticated and customized for comets than those available in the basic G-TAG simulation tool.

Scenarios implemented include the study of variations in requirements, spacecraft design (size, locations, etc. of the spacecraft components), and the environment (surface properties, slope, disturbances, etc.). The simulations, along with their visual representations

using G-View, contributed to the Comet Odyssey New Frontiers proposal effort by indicating problems and/or benefits of different approaches and designs.

This work was done by Milan Mandic, Behcet Acikmese, and Lars Blackmore of Caltech for NASA's Jet Propulsion Laboratory. Further information is contained in a TSP (see page 1).

This software is available for commercial licensing. Please contact Daniel Broderick of the California Institute of Technology at danielb@caltech.edu. Refer to NPO-47199.

Onboard Short Term Plan Viewer

Lyndon B. Johnson Space Center, Houston, Texas

Onboard Short Term Plan Viewer (OSTPV) is a computer program for electronic display of mission plans and timelines, both aboard the International Space Station (ISS) and in ISS ground control stations located in several countries. OSTPV was specifically designed both (1) for use within the limited ISS computing environment and (2) to be compatible with computers used in ground control stations. OSTPV supplants a prior system in which, aboard the ISS, timelines were printed on paper and incorporated into

files that also contained other paper documents. Hence, the introduction of OSTPV has both reduced the consumption of resources and saved time in updating plans and timelines. OSTPV accepts, as input, the mission timeline output of a legacy, print-oriented, UNIX-based program called "Consolidated Planning System" and converts the timeline information for display in an interactive, dynamic, Windows Web-based graphical user interface that is used by both the ISS crew and ground control teams in real time. OSTPV en-

ables the ISS crew to electronically indicate execution of timeline steps, launch electronic procedures, and efficiently report to ground control teams on the statuses of ISS activities, all by use of laptop computers aboard the ISS.

This work was done by Tim Hall and Troy LeBlanc of Johnson Space Center and Brian Ulman, Aaron McDonald, Paul Gramm, Li-Min Chang, Suman Keerthi, Dov Kivlovitz, and Jason Hadlock of United Space Alliance. Further information is contained in a TSP (see page 1). MSC-24335-1

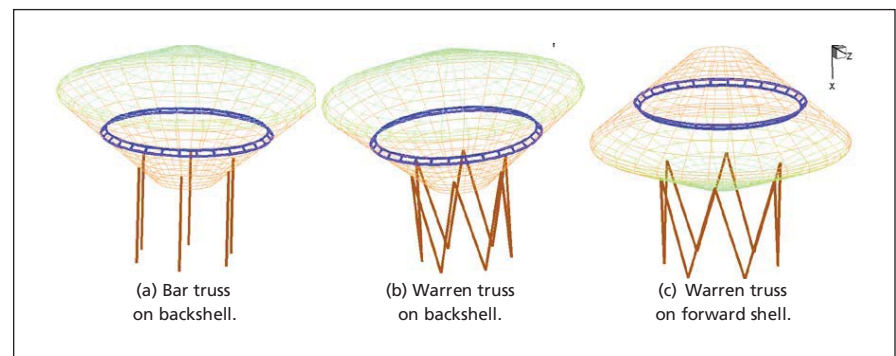
Multidisciplinary Tool for Systems Analysis of Planetary Entry, Descent, and Landing

Langley Research Center, Hampton, Virginia

Systems analysis of a planetary entry (SAPE), descent, and landing (EDL) is a multidisciplinary activity in nature. SAPE improves the performance of the systems analysis team by automating and streamlining the process, and this improvement can reduce the errors that stem from manual data transfer among discipline experts.

SAPE is a multidisciplinary tool for systems analysis of planetary EDL for Venus, Earth, Mars, Jupiter, Saturn, Uranus, Neptune, and Titan. It performs EDL systems analysis for any planet, operates cross-platform (i.e., Windows, Mac, and Linux operating systems), uses existing software components and open-source software to avoid software licensing issues, performs low-fidelity systems analysis in one hour on a computer that is comparable to an average laptop, and keeps discipline experts in the analysis loop.

SAPE uses Python, a platform-independent, open-source language, for inte-



SAPE is capable of analyzing and sizing certain classes of planetary probes, as demonstrated by sample structural topologies for Pathfinder probe.

gration and for the user interface. Development has relied heavily on the object-oriented programming capabilities that are available in Python. Modules are provided to interface with commercial and government off-the-shelf software components (e.g., thermal protection systems and finite-element analysis). SAPE cur-

rently includes the following analysis modules: geometry, trajectory, aerodynamics, aerothermal, thermal protection system, and interface for structural sizing.

This work was done by Jamshid A. Samareh of Langley Research Center. Further information is contained in a TSP (see page 1). LAR-17821-1

Bundle Security Protocol for ION

NASA's Jet Propulsion Laboratory, Pasadena, California

This software implements bundle authentication, conforming to the Delay-Tolerant Networking (DTN) Internet Draft on Bundle Security Protocol (BSP), for the Interplanetary Overlay Network (ION) implementation of

DTN. This is the only implementation of BSP that is integrated with ION.

The bundle protocol is used in DTNs that overlay multiple networks, some of which may be challenged by limitations such as intermittent and possibly unre-

dictable loss of connectivity, long or variable delay, asymmetric data rates, and high error rates. The purpose of the bundle protocol is to support interoperability across such stressed networks. The bundle protocol is layered on top of a

“convergence layer” of adapters that encapsulate bundles in the protocol data units (PDUs) of the underlying networks’ native protocols for transmission and also extract bundles from the PDUs of those protocols as they are received. This convergence-layer encapsulation enables an application in one network to communicate with an application in another network built on entirely different native protocols, both of which are spanned by the DTN.

Security will be important for the bundle protocol. The stressed environment of the underlying networks over which the bundle protocol will operate makes it important that the DTN be protected from unauthorized use, and this stressed

environment poses unique challenges on the mechanisms needed to secure the bundle protocol. Furthermore, DTNs may very likely be deployed in environments where a portion of the network might become compromised, posing the usual security challenges related to confidentiality, integrity, and availability.

The BSP encompasses four mechanisms that are designed to provide this security. The technology currently being reported implements one of those mechanisms, the Bundle Authentication Block (BAB), and provides a framework for implementation of the remaining mechanisms: Payload Integrity Block, Payload Confidentiality Block, and Extension Security Block.

The ION system runs on Linux, OS/X, Solaris, FreeBSD, RTEMS, and VxWorks, and it should port readily to other POSIX-based operating systems. No special hardware is required. RAM (random access memory) requirements depend on the volume of DTN traffic that must be handled.

This work was done by Scott C. Burleigh of Caltech and Edward J. Birrane and Christopher Krupiarz of the Johns Hopkins University Applied Physics Laboratory for NASA’s Jet Propulsion Laboratory. Further information is contained in a TSP (see page 1).

This software is available for commercial licensing. Please contact Daniel Broderick of the California Institute of Technology at danielb@caltech.edu. Refer to NPO-47211.

Visual PEF Reader — VIPER

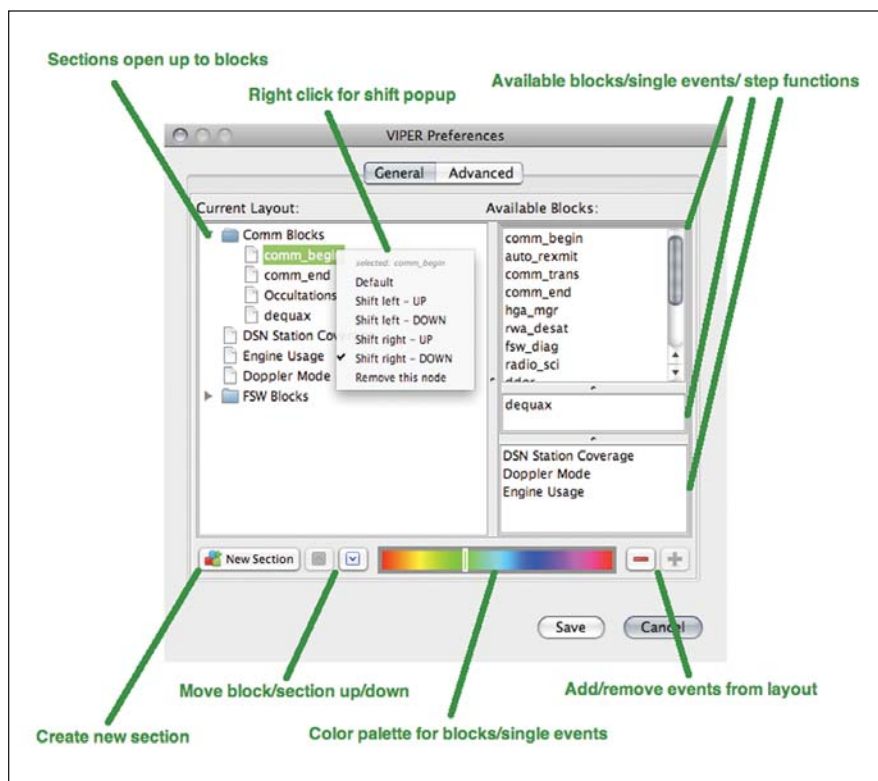
NASA’s Jet Propulsion Laboratory, Pasadena, California

This software graphically displays all pertinent information from a Predicted Events File (PEF) using the Java Swing framework, which allows for multi-platform support. The PEF is hard to weed through when looking for specific information and it is a desire for the MRO (Mars Reconnaissance Orbiter) Mission Planning & Sequencing Team (MPST) to have a different way to visualize the data. This tool will provide the team with a visual way of reviewing and error-checking the sequence product.

The front end of the tool contains much of the aesthetically appealing material for viewing. The time stamp is displayed in the top left corner, and highlighted details are displayed in the bottom left corner. The time bar stretches along the top of the window, and the rest of the space is allotted for blocks and step functions. A preferences window is used to control the layout of the sections along with the ability to choose color and size of the blocks.

Double-clicking on a block will show information contained within the block. Zooming into a certain level will graphically display that information as an overlay on the block itself. Other functions include using hotkeys to navigate, an option to jump to a specific time, enabling a vertical line, and double-clicking to zoom in/out.

The back end involves a configuration file that allows a more experienced user to pre-define the structure of a block, a single event, or a step function. The individual will have to



VIPER GUI general preferences.

determine what information is important within each block and what actually defines the beginning and end of a block. This gives the user much more flexibility in terms of what the tool is searching for. In addition to the configurability, all the settings in the preferences window are saved in the configuration file as well.

This work was done by Victor Luo, Teerapat Khanampornpan, Rudy A. Boehmer, and Rachel Y. Kim of Caltech for NASA’s Jet Propulsion Laboratory. Further information is contained in a TSP (see page 1).

This software is available for commercial licensing. Please contact Daniel Broderick of the California Institute of Technology at danielb@caltech.edu. Refer to NPO-47509.

Link Analysis in the Mission Planning Lab

Goddard Space Flight Center, Greenbelt, Maryland

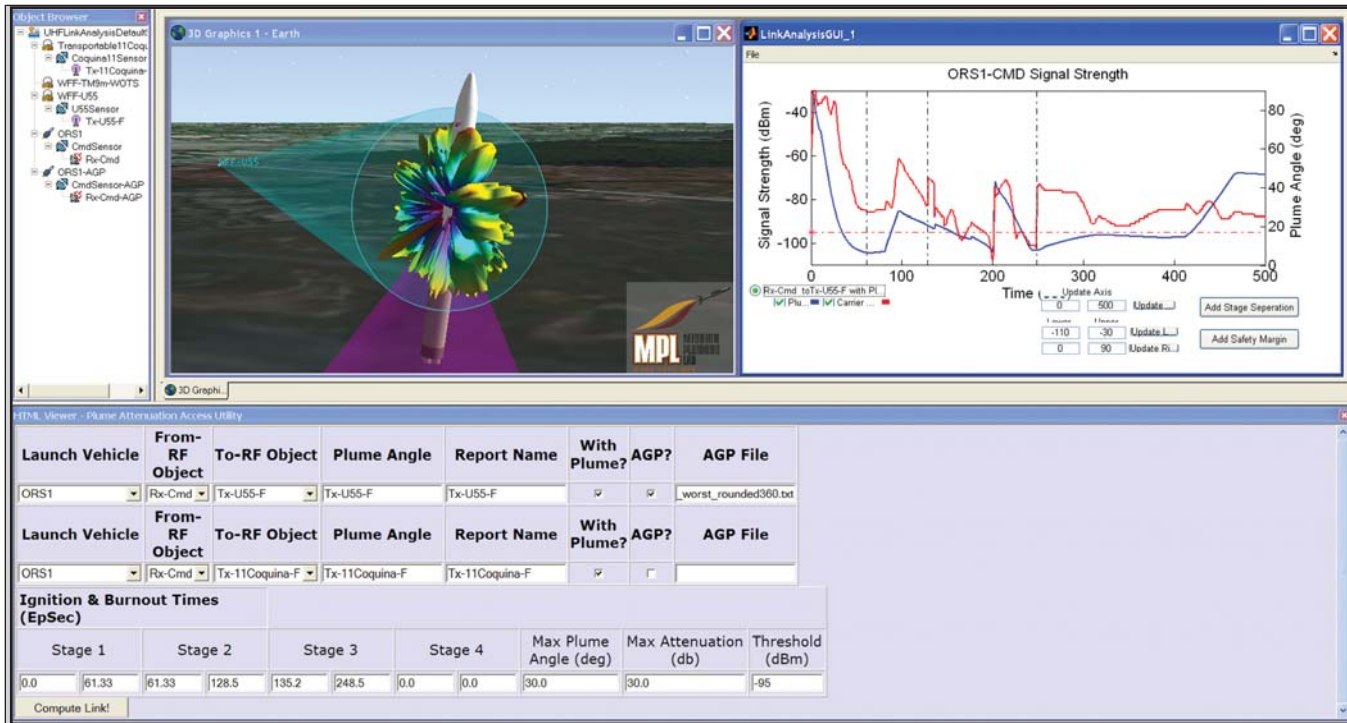
The legacy communications link analysis software currently used at Wallops Flight Facility involves processes that are different for command destruct, radar, and telemetry. There is a clear advantage to developing an easy-to-use tool that combines all the processes in one application. Link Analysis in the Mission Planning Lab (MPL) uses custom software and algorithms integrated with Analytical Graphics Inc. Satellite Toolkit (AGI STK). The MPL link analysis tool uses pre/post-mission data to conduct a dynamic link analysis between ground assets and the launch vehicle. Just as the legacy methods do, the MPL link analysis

tool calculates signal strength and signal-to-noise according to the accepted processes for command destruct, radar, and telemetry assets. Graphs and other custom data are generated rapidly in formats for reports and presentations. STK is used for analysis as well as to depict plume angles and antenna gain patterns in 3D.

The MPL has developed two interfaces with the STK software (see figure). The first interface is an HTML utility, which was developed in Visual Basic to enhance analysis for plume modeling and to offer a more user friendly, flexible tool. A graphical user interface

(GUI) written in MATLAB (see figure upper right-hand corner) is also used to quickly depict link budget information for multiple ground assets. This new method yields a dramatic decrease in the time it takes to provide launch managers with the required link budgets to make critical pre-mission decisions. The software code used for these two custom utilities is a product of NASA's MPL.

This work was done by Jessica A. McCarthy, Benjamin W. Cervantes, Sarah C. Daugherty, Felipe Arroyo, and Divyang Mago of Goddard Space Flight Center. Further information is contained in a TSP (see page 1). GSC-15733-1



Mission Planning Lab Link analysis software tool.

MatchGUI: A Graphical MATLAB-Based Tool for Automatic Image Co-Registration

NASA's Jet Propulsion Laboratory, Pasadena, California

MatchGUI software, based on MATLAB, automatically matches two images and displays the match result by superimposing one image on the other. A slider bar allows focus to shift between the two images. There are tools for zoom, auto-crop to overlap region, and basic image markup. Given a pair of

ortho-rectified images (focused primarily on Mars orbital imagery for now), this software automatically co-registers the imagery so that corresponding image pixels are aligned. MatchGUI requires minimal user input, and performs a registration over scale and in-plane rotation fully automatically.

This work was done by Adnan I. Ansar of Caltech for NASA's Jet Propulsion Laboratory. For more information, contact iaoffice@jpl.nasa.gov.

This software is available for commercial licensing. Please contact Daniel Broderick of the California Institute of Technology at danielb@caltech.edu. Refer to NPO-47513.

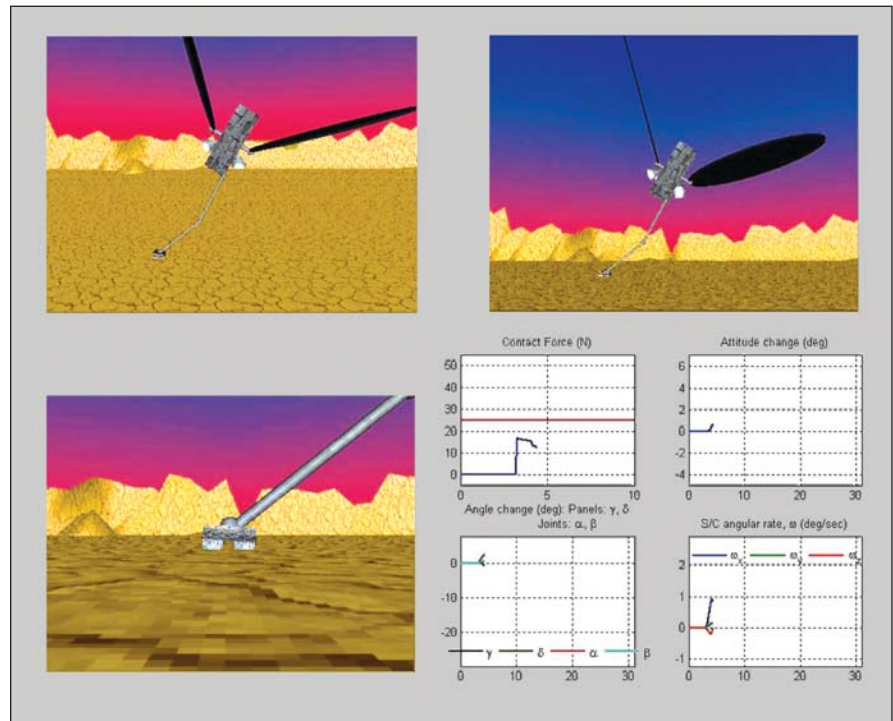
Spacecraft Guidance, Navigation, and Control Visualization Tool

NASA's Jet Propulsion Laboratory, Pasadena, California

G-View is a 3D visualization tool for supporting spacecraft guidance, navigation, and control (GN&C) simulations relevant to small-body exploration and sampling (see figure). The tool is developed in MATLAB using Virtual Reality Toolbox and provides users with the ability to visualize the behavior of their simulations, regardless of which programming language (or machine) is used to generate simulation results. The only requirement is that multi-body simulation data is generated and placed in the proper format before applying G-View.

G-View allows the user to visualize the behavior of a multi-body system (i.e. a spacecraft, the translations and rotations of the spacecraft body components, thruster firings, and thrust magnitude) by simultaneously showing plots of various relevant states and parameters. In G-View, the user can easily manipulate the location, zoom, translation, and direction of the camera, thus providing a wide range of options for viewing the behavior of specific spacecraft components, such as the solar panels, mechanical arms, brush-wheel sampler, joints, etc.

G-View is easily modifiable and can be adjusted to specific design or simulation requirements. For example, one mode of usage is to create movie clips for a batch-collected set of data. This provides a visual aid supporting iterative design methods and an efficient tool for generating presentations. G-View can also be applied to a computer



Comet GN&C example of G-View.

simulation one frame at a time. This is especially beneficial when applied to simulation environments that require long running times. By extracting visualization data at specific time instants, the user can assess whether the simulation has the desired behavior or if something is wrong and is not worth continuing. In this manner, G-View can save significant time when simulating

complex scenarios, and improve troubleshooting efficiency.

This work was done by Milan Mandic, Behcet Acikmese, and Lars Blackmore of Caltech for NASA's Jet Propulsion Laboratory. Further information is contained in a TSP (see page 1).

This software is available for commercial licensing. Please contact Daniel Broderick of the California Institute of Technology at danielb@caltech.edu. Refer to NPO-47197.

Mission Operations Planning and Scheduling System (MOPSS)

Goddard Space Flight Center, Greenbelt, Maryland

MOPSS is a generic framework that can be configured on the fly to support a wide range of planning and scheduling applications. It is currently used to support seven missions at Goddard Space Flight Center (GSFC) in roles that include science planning, mission planning, and real-time control.

Prior to MOPSS, each spacecraft project built its own planning and scheduling capability to plan satellite activities and communications and to create the commands to be uplinked to the space-

craft. This approach required creating a data repository for storing planning and scheduling information, building user interfaces to display data, generating needed scheduling algorithms, and implementing customized external interfaces. Complex scheduling problems that involved reacting to multiple variable situations were analyzed manually. Operators then used the results to add commands to the schedule. Each architecture was unique to specific satellite requirements.

MOPSS is an expert system that automates mission operations and frees the flight operations team to concentrate on critical activities. It is easily reconfigured by the flight operations team as the mission evolves. The heart of the system is a custom object-oriented data layer mapped onto an Oracle relational database. The combination of these two technologies allows a user or system engineer to capture any type of scheduling or planning data in the system's generic data storage via a GUI.

MOPSS uses CORBA in conjunction with a multi-tier architecture to allow multiple users to concurrently view and edit schedule data. The adaptable architecture of MOPSS also enables easy integration of tools and models to satisfy new system requirements. MOPSS has two clients: an X/MOTIF client and a Java client. The Java client is effective over the Web and has been used by remote MAP

mission scientists and engineers to monitor spacecraft integration tests.

The most obvious use of MOPSS is for control of commercial satellites. In the television industry, MOPSS could be used to schedule TV commercials on broadcast television based on FCC rules, demographics, and program content. In the medical field, MOPSS could be used to schedule and optimize use of hospitals

in a network and resources within hospitals. In the power industry, MOPSS can be used to schedule nuclear power plant maintenance. The education and transportation fields are also candidates.

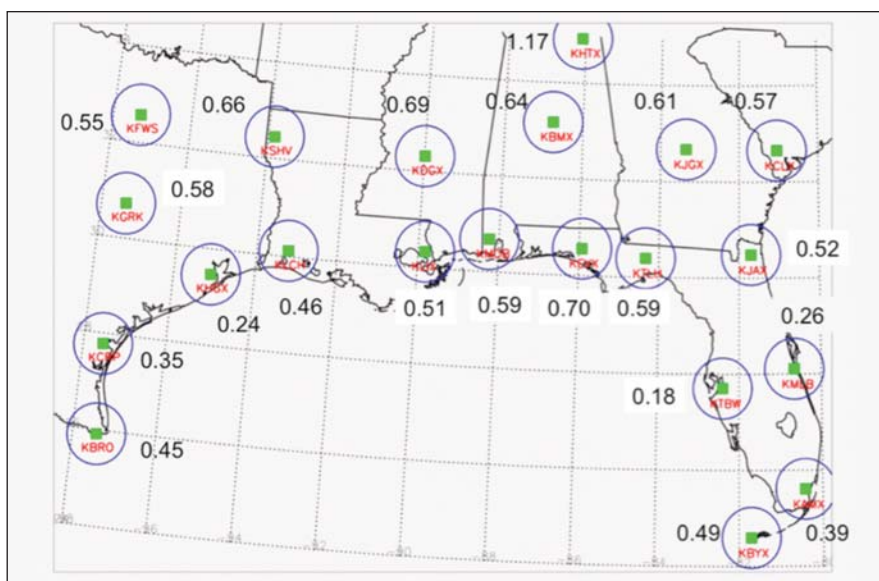
This work was done by Terri Wood of Goddard Space Flight Center and Paul Hempel of Computer Sciences Corp. Further information is contained in a TSP (see page 1).. GSC-15858-1

Global Precipitation Mission Visualization Tool

Goddard Space Flight Center, Greenbelt, Maryland

The Global Precipitation Mission (GPM) software provides graphic visualization tools that enable easy comparison of ground- and space-based radar observations. It was initially designed to compare ground radar reflectivity from operational, ground-based, S- and C-band meteorological radars with comparable measurements from the Tropical Rainfall Measuring Mission (TRMM) satellite's precipitation radar instrument. This design is also applicable to other ground-based and space-based radars, and allows both ground- and space-based radar data to be compared for validation purposes.

The tool creates an operational system that routinely performs several steps. It ingests satellite radar data (precipitation radar data from TRMM) and ground-based meteorological radar data from a number of sources. Principally, the ground radar data comes from national networks of weather radars (see figure). The data ingested by the visualization tool must conform to the data formats used in GPM Validation Network Geometry-matched data product generation. The software also performs match-ups of the radar volume data for the ground- and space-based data, as



Location of Validation Network match-up sites and associated site grid domains in the southeastern U.S.

well as statistical and graphical analysis (including two-dimensional graphical displays) on the match-up data.

The visualization tool software is written in IDL, and can be operated either in the IDL development environment or

as a stand-alone executable function.

This work was done by Mathew Schwaller of Goddard Space Flight Center. For further information, contact the Goddard Innovative Partnerships Office at (301) 286-5810. GSC-15785-1

Thermal Protection System Imagery Inspection Management System —TIIMS

Lyndon B. Johnson Space Center, Houston, Texas

TIIMS is used during the inspection phases of every mission to provide quick visual feedback, detailed inspection data, and determination to the mission management team. This system consists of a visual Web page interface, an SQL database, and a graphical image generator. These combine to allow a user to as-

certain quickly the status of the inspection process, and current determination of any problem zones.

The TIIMS system allows inspection engineers to enter their determinations into a database and to link pertinent images and video to those database entries. The database then assigns criteria to

each zone and tile, and via query, sends the information to a graphical image generation program. Using the official TIPS database tile positions and sizes, the graphical image generation program creates images of the current status of the orbiter, coloring zones, and tiles based on a predefined key code. These

images are then displayed on a Web page using customized JAVA scripts to display the appropriate zone of the orbiter based on the location of the user's cursor. The close-up graphic and database entry for that particular zone can then be seen by selecting the zone. This page

contains links into the database to access the images used by the inspection engineer when they make the determination entered into the database. Status for the inspection zones changes as determinations are refined and shown by the appropriate color code.

This work was done by Sharon Goza and David L. Melendrez of Johnson Space Center, Marsha Hennigan of Jacobs Engineering, Daniel LaBasse of MEI Technologies, and Daniel J. Smith, consultant. Further information is contained in a TSP (see page 1). MSC-24484-1

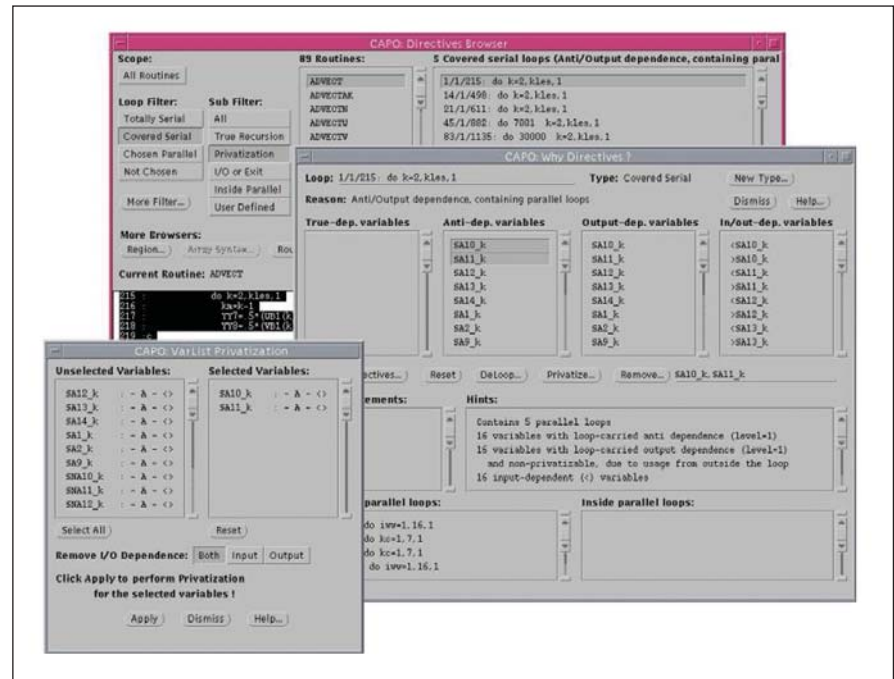
Computer-Aided Parallelizer and Optimizer

Ames Research Center, Moffett Field, California

The Computer-Aided Parallelizer and Optimizer (CAPO) automates the insertion of compiler directives (see figure) to facilitate parallel processing on Shared Memory Parallel (SMP) machines. While CAPO currently is integrated seamlessly into CAPTools (developed at the University of Greenwich, now marketed as ParaWise), CAPO was independently developed at Ames Research Center as one of the components for the Legacy Code Modernization (LCM) project. The current version takes serial FORTRAN programs, performs interprocedural data dependence analysis, and generates OpenMP directives. Due to the widely supported OpenMP standard, the generated OpenMP codes have the potential to run on a wide range of SMP machines.

CAPO relies on accurate interprocedural data dependence information currently provided by CAPTools. Compiler directives are generated through identification of parallel loops in the outermost level, construction of parallel regions around parallel loops and optimization of parallel regions, and insertion of directives with automatic identification of private, reduction, induction, and shared variables.

Attempts also have been made to identify potential pipeline parallelism (implemented with point-to-point syn-



The Main GUI (Directives Browser) for CAPO.

chronization). Although directives are generated automatically, user interaction with the tool is still important for producing good parallel codes. A comprehensive graphical user interface is included for users to interact with the parallelization process.

The work was done by Haoqiang Jin of MRJ Technology Solutions for Ames Research Center. For further information, access <http://people.nasa.gov/~hjin/CAPO/index.html>. ARC-14487-1

CCSDS Advanced Orbiting Systems Virtual Channel Access Service for QoS MACHETE Model

NASA's Jet Propulsion Laboratory, Pasadena, California

To support various communications requirements imposed by different missions, interplanetary communication protocols need to be designed, validated, and evaluated carefully. Multi-mission Advanced Communications Hybrid Environment for Test and

Evaluation (MACHETE), described in "Simulator of Space Communication Networks" (NPO-41373), *NASA Tech Briefs*, Vol. 29, No. 8 (August 2005), p. 44, combines various tools for simulation and performance analysis of space networks. The MACHETE environment

supports orbital analysis, link budget analysis, communications network simulations, and hardware-in-the-loop testing. By building abstract behavioral models of network protocols, one can validate performance after identifying the appropriate metrics of interest. The

innovators have extended the MACHETE model library to include a generic link-layer Virtual Channel (VC) model supporting quality-of-service (QoS) controls based on IP streams.

The main purpose of this generic Virtual Channel model addition was to interface fine-grain flow-based QoS (quality of service) between the network and MAC layers of the QualNet simulator, a commercial component of MACHETE. This software model adds the capability of mapping IP streams, based on header fields, to virtual channel num-

bers, allowing extended QoS handling at link layer. This feature further refines the QoS v existing at the network layer.

QoS at the network layer (e.g. diff-serv) supports few QoS classes, so data from one class will be aggregated together; differentiating between flows internal to a class/priority is not supported. By adding QoS classification capability between network and MAC layers through VC, one maps multiple VCs onto the same physical link. Users then specify different VC weights, and

different queuing and scheduling policies at the link layer. This VC model supports system performance analysis of various virtual channel link-layer QoS queuing schemes independent of the network-layer QoS systems.

This work was done by Esther H. Jennings and John S. Segui of Caltech for NASA's Jet Propulsion Laboratory. For more information, contact iaoffice@jpl.nasa.gov.

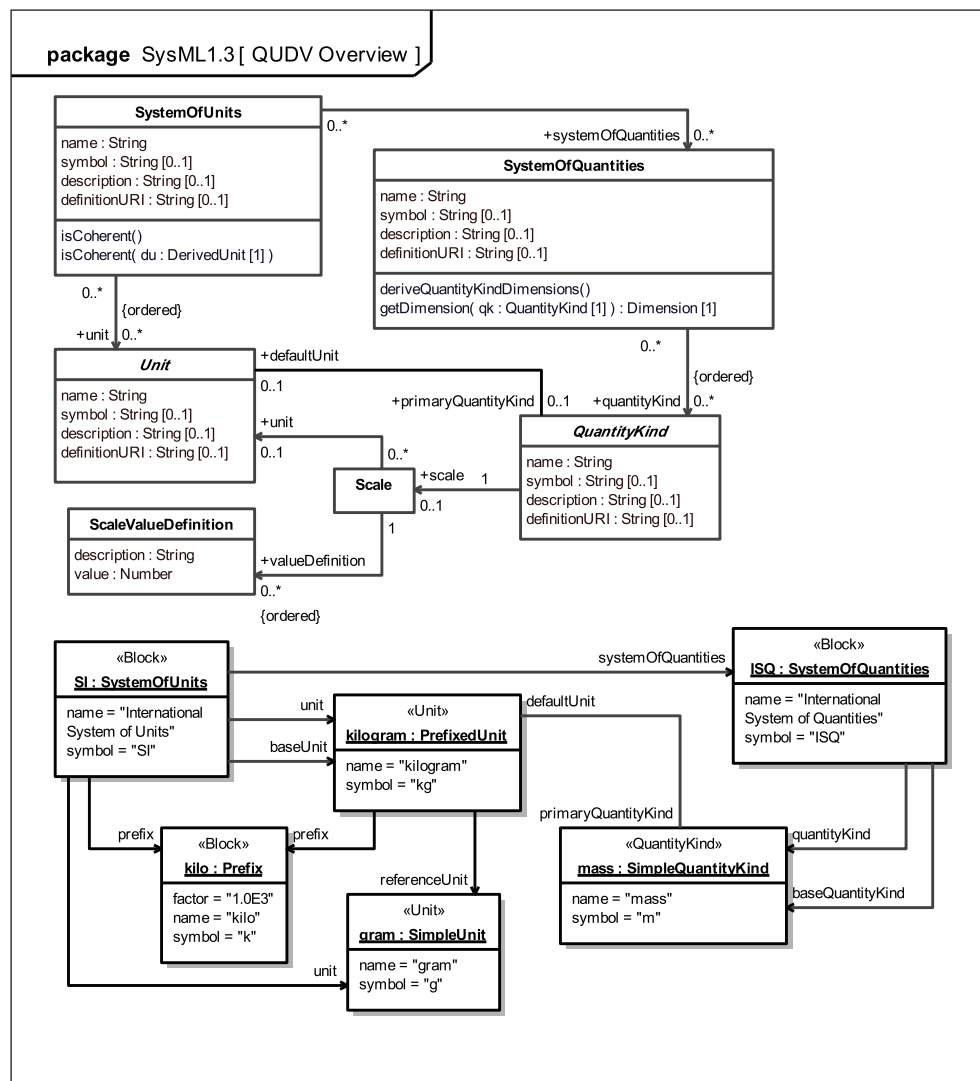
This software is available for commercial licensing. Please contact Daniel Broderick of the California Institute of Technology at danielb@caltech.edu. Refer to NPO-47464.

Conceptual Model of Quantities, Units, Dimensions, and Values

NASA's Jet Propulsion Laboratory, Pasadena, California

JPL collaborated with experts from industry and other organizations to develop a conceptual model of quantities, units, dimensions, and values based on the current work of the ISO 80000 committee revising the International System of Units & Quantities based on the International Vocabulary of Metrology (VIM). By providing support for ISO 80000 in SysML via the International Vocabulary of Metrology (VIM), this conceptual model provides, for the first time, a standard-based approach for addressing issues of unit coherence and dimensional analysis into the practice of systems engineering with SysMLbased tools. This conceptual model provides support for two kinds of analyses specified in the International Vocabulary of Metrology (VIM): coherence of units as well as of systems of quantities.

To provide a solid and stable foundation, the model for defining quantities, units, dimensions, and values in SysML is explicitly based on the concepts defined in VIM. At the same time, the model library is designed in such a way that extensions to the ISQ (International System of Quantities) and SI Units (Système International d'Unités) can be represented, as well as any alternative systems of quantities and units.



The key abstractions defined in the conceptual model of **Quantities, Units, Dimensions and Values (QUDV)** based on normative references in ISO 80000-1:2009, and an excerpt of its application for the SI Units and Quantities as defined in ISO 80000-1:2009, in NIST's Reference on Constants, Units and Uncertainty, and in the IEEE/ASTM American National Standards for Metric Practice SI-10™ 2010.

The model library can be used to support SysML user models in various ways. A simple approach is to define and document libraries of reusable systems of units and quantities for reuse across multiple projects, and to link units and quantity kinds from these libraries to

Unit and QuantityKind stereotypes defined in SysML user models.

This work was done by Nicolas F. Rouquette of Caltech, Hans-Peter DeKoenig of the European Space Agency, Roger Burkhardt of Deere & Company, and Huascar Espinoza of the French Centre of Atomic Energy for

NASA's Jet Propulsion Laboratory. For more information, contact iaoffice@jpl.nasa.gov.

The software used in this innovation is available for commercial licensing. Please contact Daniel Broderick of the California Institute of Technology at danielb@caltech.edu. Refer to NPO-47251.

Sptrace

NASA's Jet Propulsion Laboratory, Pasadena, California

Sptrace is a general-purpose space utilization tracing system that is conceptually similar to the commercial "Purify" product used to detect leaks and other memory usage errors. It is designed to monitor space utilization in any sort of "heap," i.e., a region of data storage on some device (nominally memory; possibly shared and possibly persistent) with a flat address space. This software can trace usage of shared and/or non-volatile storage in addition to private RAM (random access memory).

Sptrace is implemented as a set of C function calls that are invoked from within the software that is being examined. The function calls fall into two broad classes: (1) functions that are embedded within the heap management software [e.g., JPL's SDR (Simple Data Recorder) and PSM (Personal Space Management) systems] to enable heap usage analysis by populating a virtual time-sequenced "log" of usage activity, and (2) reporting functions that are embedded within the application program whose behavior is suspect. For ease of

use, these functions may be wrapped privately inside public functions offered by the heap management software. Sptrace can be used for VxWorks or RTEMS real-time systems as easily as for Linux or OS/X systems.

This work was done by Scott C. Burleigh of ACRO for NASA's Jet Propulsion Laboratory. Further information is contained in a TSP (see page 1).

This software is available for commercial licensing. Please contact Daniel Broderick of the California Institute of Technology at danielb@caltech.edu. Refer to NPO-41626.

S-Band POSIX Device Drivers for RTEMS

NASA's Jet Propulsion Laboratory, Pasadena, California

This is a set of POSIX device driver level abstractions in the RTEMS RTOS (Real-Time Executive for Multiprocessor Systems real-time operating system) to S-Band radio hardware devices that have been instantiated in an FPGA (field-programmable gate array). These include A/D (analog-to-digital) sample capture, D/A (digital-to-analog) sample playback, PLL (phase-locked-loop) tuning, and PWM (pulse-width-modulation)-controlled gain. This software interfaces to S-band radio hardware in an attached Xilinx

Virtex-2 FPGA. It uses plug-and-play device discovery to map memory to device IDs. Instead of interacting with hardware devices directly, using direct-memory mapped access at the application level, this driver provides an application programming interface (API) offering that easily uses standard POSIX function calls. This simplifies application programming, enables portability, and offers an additional level of protection to the hardware.

There are three separate device drivers included in this package: `sband_device`

(ADC capture and DAC playback), `pll_device` (RF front end PLL tuning), and `pwm_device` (RF front end AGC control).

This work was done by James P. Lux, Minh Lang, Kenneth J. Peters, and Gregory H. Taylor of Caltech for NASA's Jet Propulsion Laboratory. For more information, contact iaoffice@jpl.nasa.gov.

This software is available for commercial licensing. Please contact Daniel Broderick of the California Institute of Technology at danielb@caltech.edu. Refer to NPO-47496.

MaROS: Information Management Service

NASA's Jet Propulsion Laboratory, Pasadena, California

This software is provided by the Mars Relay Operations Service (MaROS) task to a variety of Mars projects for the purpose of coordinating communications sessions between landed spacecraft assets and orbiting spacecraft assets at Mars. The Information Management Service centralizes a set of functions

previously distributed across multiple spacecraft operations teams, and as such, greatly improves visibility into the end-to-end strategic coordination process. Most of the process revolves around the scheduling of communications sessions between the spacecraft during periods of time when a landed

asset on Mars is geometrically visible by an orbiting spacecraft. These "relay" sessions are used to transfer data both to and from the landed asset via the orbiting asset on behalf of Earth-based spacecraft operators.

This software component is an application process running as a Java virtual

machine. The component provides all service interfaces via a Representational State Transfer (REST) protocol over “https” to external clients. There are two general interaction modes with the service: upload and download of data. For data upload, the service must execute logic specific to the upload data type and trigger any applicable calculations including pass delivery latencies and overflight conflicts. For data download, the software must retrieve and correlate

requested information and deliver to the requesting client.

The provision of this service enables several key advancements over legacy processes and systems. For one, this service represents the first time that end-to-end relay information is correlated into a single shared repository. The software also provides the first multimission latency calculator; previous latency calculations had been performed on a mission-by-mission basis.

This work was done by Daniel A. Allard, Roy E. Gladden, Jesse J. Wright, Franklin H. Hy, Gregg R. Rabideau, and Michael N. Wallick of Caltech for NASA’s Jet Propulsion Laboratory. Further information is contained in a TSP (see page 1).

This software is available for commercial licensing. Please contact Daniel Broderick of the California Institute of Technology at danielb@caltech.edu. Refer to NPO-47454.

Interplanetary Overlay Network Bundle Protocol Implementation

NASA’s Jet Propulsion Laboratory, Pasadena, California

The Interplanetary Overlay Network (ION) system’s BP package, an implementation of the Delay-Tolerant Networking (DTN) Bundle Protocol (BP) and supporting services, has been specifically designed to be suitable for use on deep-space robotic vehicles. Although the ION BP implementation is unique in its use of zero-copy objects for high performance, and in its use of resource-sensitive rate control, it is fully interoperable with other implementations of the BP specification (Internet RFC 5050).

The ION BP implementation is built using the same software infrastructure that underlies the implementation of the CCSDS (Consultative Committee for Space Data Systems) File Delivery Protocol (CFDP) built into the flight software

of Deep Impact. It is designed to minimize resource consumption, while maximizing operational robustness. For example, no dynamic allocation of system memory is required. Like all the other ION packages, ION’s BP implementation is designed to port readily between Linux and Solaris (for easy development and for ground system operations) and VxWorks (for flight systems operations). The exact same source code is exercised in both environments.

Initially included in the ION BP implementations are the following: libraries of functions used in constructing bundle forwarders and convergence-layer (CL) input and output adapters; a simple prototype bundle forwarder and associated CL adapters designed to run over an IP-

based local area network; administrative tools for managing a simple DTN infrastructure built from these components; a background daemon process that silently destroys bundles whose time-to-live intervals have expired; a library of functions exposed to applications, enabling them to issue and receive data encapsulated in DTN bundles; and some simple applications that can be used for system check-out and benchmarking.

This work was done by Scott C. Burleigh of ARCO for NASA’s Jet Propulsion Laboratory. Further information is contained in a TSP (see page 1).

This software is available for commercial licensing. Please contact Daniel Broderick of the California Institute of Technology at danielb@caltech.edu. Refer to NPO-41628.

STRS SpaceWire FPGA Module

NASA’s Jet Propulsion Laboratory, Pasadena, California

An FPGA module leverages the previous work from Goddard Space Flight Center (GSFC) relating to NASA’s Space Telecommunications Radio System (STRS) project. The STRS SpaceWire FPGA Module is written in the Verilog Register Transfer Level (RTL) language, and it encapsulates an unmodified GSFC core (which is written in VHDL). The module has the necessary inputs/outputs (I/Os) and parameters to integrate seamlessly with the SPARC I/O FPGA Interface module (also developed for the STRS operating environment, OE).

Software running on the SPARC processor can access the configuration

and status registers within the SpaceWire module. This allows software to control and monitor the SpaceWire functions, but it is also used to give software direct access to what is transmitted and received through the link. SpaceWire data characters can be sent/received through the software interface, as well as through the dedicated interface on the GSFC core. Similarly, SpaceWire time codes can be sent/received through the software interface or through a dedicated interface on the core.

This innovation is designed for plug-and-play integration in the STRS OE. The SpaceWire module simplifies the in-

terfaces to the GSFC core, and synchronizes all I/O to a single clock. An interrupt output (with optional masking) identifies time-sensitive events within the module. Test modes were added to allow internal loopback of the SpaceWire link and internal loopback of the client-side data interface.

This work was done by James P. Lux, Gregory H. Taylor, Minh Lang, and Ryan A. Stern of Caltech for NASA’s Jet Propulsion Laboratory. For more information, contact iaoffice@jpl.nasa.gov.

This software is available for commercial licensing. Please contact Daniel Broderick of the California Institute of Technology at danielb@caltech.edu. Refer to NPO-47434.



Geodetic Strain Analysis Tool

NASA's Jet Propulsion Laboratory, Pasadena, California

A geodetic software analysis tool enables the user to analyze 2D crustal strain from geodetic ground motion, and create models of crustal deformation using a graphical interface. Users can use any geodetic measurements of ground motion and derive the 2D crustal strain interactively. This software also provides a forward-modeling tool that calculates a geodetic velocity and strain field for a given fault model, and lets the user compare the modeled strain field with the strain field obtained from the user's data.

Users may change parameters "on-the-fly" and obtain a real-time recalculation of the resulting strain field. Four data products are computed: maximum

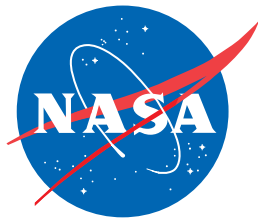
shear, dilatation, shear angle, and principal components. The current view and data dependencies are processed first. The remaining data products and views are then computed in a round-robin fashion to anticipate view changes. When an analysis or display parameter is changed, the affected data products and views are invalidated and progressively re-displayed as available.

This software is designed to facilitate the derivation of the strain fields from the GPS and strain meter data that sample it to facilitate the understanding of the strengths and weaknesses of the strain field derivation from continuous GPS (CGPS) and other geodetic data from a variety of tectonic settings, to

converge on the "best practices" strain derivation strategy for the Solid Earth Science ESDR System (SESES) project given the CGPS station distribution in the western U.S., and to provide SESES users with a scientific and educational tool to explore the strain field on their own with user-defined parameters.

This work was done by Sharon Kedar, Sean C. Baxter, Jay W. Parker, Frank H. Webb, Susan E. Owen, Anthony J. Sibthorpe, and Danan Dong of Caltech for NASA's Jet Propulsion Laboratory. Further information is contained in a TSP (see page 1).

This software is available for commercial licensing. Please contact Daniel Broderick of the California Institute of Technology at danielb@caltech.edu. Refer to NPO-47504.



National Aeronautics and
Space Administration